NUREG
SAND[illegible]-1043
R7
Printed March 1987

Coolability of Stratified UO_2 Debris in Sodium With Downward Heat Removal: The D13 Experiment

C. A. Ottinger, G. W. Mitchell, A. W. Reed, H. Meister

Prepared by
Sandia National Laboratories
Albuquerque, New Mexico 87185 and Livermore, California 94550
for the United States Department of Energy
under Contract DE-AC04-76DP00789

Prepared for
U. S. NUCLEAR REGULATORY COMMISSION

SF2900Q(8-81)

DISCLAIMER

Available from

Superintendent of Documents
U.S. Government Printing Office
Post Office Box 37082
Washington, D.C. 20013-7082

and

National Technical Information Service
Springfield, VA 22161

NUREG/CR-4719
SAND86-1043
R7

NUREG/CR--4719

TI87 010031

COOLABILITY OF STRATIFIED UO_2 DEBRIS IN SODIUM WITH DOWNWARD HEAT REMOVAL: THE D13 EXPERIMENT*

C. A. Ottinger
G. W. Mitchell
A. W. Reed
H. Meister**

March 1987

Sandia National Laboratories
Albuquerque, NM 87185
Operated by
Sandia Corporation
for the
U.S. Department of Energy

Prepared for
Accident Evaluation Branch
Office of Nuclear Research
U.S. Nuclear Regulatory Commission
Washington, DC 20555
Under Memorandum of Understanding DOE 40-550-75
NRC FIN A1181

* This work was supported by the U.S. Nuclear Regulatory Commission, EURATOM JRC, and the Japanese PNC and performed at Sandia National Laboratories.
** EURATOM Joint Research Center, Ispra, Italy

ABSTRACT

The LMFBR Debris Coolability Program at Sandia National Laboratories investigates the coolability of particle beds that may form following a severe accident involving core disassembly in a nuclear reactor. The D series experiments utilize fission heating of fully enriched UO_2 particles submerged in sodium to realistically simulate decay heating. The D13 experiment is the first in the series to study the effects of bottom cooling of stratified debris, which could be provided in an actual accident condition by structural materials onto which the debris might settle. Additionally, the D13 experiment was designed to achieve maximum temperatures in the debris approaching the melting point of UO_2. The experiment was operated for over 40 hours and investigated downward heat removal at specific powers of 0.22 to 2.58 W/g. Channeled dryout in the debris was achieved at powers from 0.94 to 2.58 W/g. Maximum temperatures approaching 2700°C were attained. Bottom heat removal was up to 750 kW/m^2 as compared to 450 kW/m^2 in the D10 experiment.

CONTENTS

LIST OF FIGURES

LIST OF TABLES

ACKNOWLEDGMENT

The operation of the D13 experiment was preceded by over three years of concept formulation, design engineering, hardware testing, component fabrication and assembly of the experiment. A large number of individuals were involved in the project over these three years and deserve substantial recognition for their efforts. J. Gronager, D. Cox, K. Takahashi (PNC), and G. Fieg (KfK) initiated the preliminary concepts and design including fabrication and operation of a full-scale systems test of the experiment, which contributed substantially to subsequent design efforts. Fabrication of many complex experimental components was ably guided by K. Gawith. The efforts of R. Gomez during fabrication and assembly and of J. Reinhart and H. Heerdt during final preparation and operation were essential to the conduct of the experiment.

Thanks also to R. Lipinski, J. Kelly, K. Mehr (JRC Ispra), and L. Barleon (KfK) for their insight, analyses, and contributions prior to and during operation of the experiment. Finally, thanks to T. Schmidt and J. Walker for their support and supervision during difficult times.

1. INTRODUCTION

The LMFBR Debris Coolability Program at Sandia National Laboratories investigates the coolability of particle beds that may form following a severe accident involving core disassembly in a nuclear reactor. This debris is capable of generating significant power through the decay of fission products. If the debris is flooded with coolant, heat removal can occur by conduction, convection, and boiling of the coolant. If the decay heat power is sufficiently high, dryout may occur, preventing the entry of liquid into regions of the bed. Because heat removal is then limited to conduction by solid UO_2 and vapor phases and by radiation, the temperatures in the dry regions of the bed increase considerably, which may threaten underlying structural components.

The Debris Coolability Program is a USNRC, Joint Research Center Ispra (EURATOM) and Power Reactor and Nuclear Fuel Development Corporation (PNC) of Japan jointly sponsored series of experiments which are designed to investigate the coolability of fragmented reactor materials. The D series experiments utilize fission heating of fully enriched UO_2 particles in the Annular Core Research Reactor (ACRR) to realistically simulate decay heat. Sodium is used as the coolant to study the effects of liquid subcooling with a high conductivity fluid. The experiments conducted to date have investigated the parameters of bed depth, subcooling, particle size distribution, and stratification.[1-5] The debris has been insulated on the sides and the bottom, with the exception of D10,[6] to allow one-dimensional analysis of the results. Additionally, with the exception of the D10 experiment, tests accomplished to date have been limited to maximum temperatures of about 1200°C based on the utilization of conventional materials. Although these experiments are directed primarily toward Liquid Metal Fast Breeder Reactor safety questions, the coolability models that have been developed based on these experiments are applicable to both sodium and water cooled reactors.

The D10 experiment[6] was the first in the series to study the effects of bottom cooling which might be provided by structural materials onto which the reactor debris might settle in an accident condition. It was designed to achieve temperatures in the debris approaching the melting point of UO_2 to investigate any change in coolability which might occur at those temperatures. D13 was identical in design to the D10 experiment but incorporated a stratified rather than a uniformly mixed particle bed. The experiment was operated for over 40 hours. Downward cooling in a stratified bed was investigated under subcooled and disturbed (partially channeled) bed conditions. Extended dryouts were established with maximum temperatures in the bed of >2700°C.

This report is intended to be primarily a description of the operation of the experiment and a compilation of the data. Only limited interpretation and analysis of the results are provided.

2. EXPERIMENT DESCRIPTION

2.1 Experimental Objectives

The primary objective of the D series experiments is to provide a data base for the development and validation of models that can be used to assess reactor safety. Thus, the experiments cover as wide a parameter space as possible and attempt to identify the important phenomena that govern coolability. The D10 and D13 experiments were originally proposed in 1979 as the first in-pile experiments investigating debris coolability that would include the effects of bottom cooling of the debris. This would simulate the cooling that could be provided by structural components onto which the debris might settle in an accident. The objectives of the experiment were later expanded to include the investigation of effects that might be induced at high temperatures as the debris approaches UO_2 melt. Based on these objectives, the experiment was designed to study the coolability of a stratified bed of UO_2 particles in sodium, 160 mm high and 102 mm in diameter, which could be fission heated in the ACRR to a maximum temperature of 2500°C and a maximum power of about 2 W/g in the UO_2.

To achieve these objectives, temperatures were recorded at different power levels to study various regimes of heat removal that might exist in such a bed. Power required to produce incipient dryout at various rates of downward cooling were determined during the experiment. Additionally, the thermal conductivity of dry debris in the presence of sodium vapor at power levels above that required for incipient dryout can be determined based on measured temperatures.

2.2 Experiment Design

The design of the D13 experiment proceeded in parallel with the D10 experiment and is described in Reference 6. Most of the design information is available in that reference and will not be repeated here. The experiment section (Figure 1) consists of the lower 200 cm of the assembly installed in the 23-cm diameter dry central cavity of the ACRR as shown in Figure 2. The bed was contained in a double-walled crucible, which was side insulated to provide an approximate one-dimensional geometry for analysis and to insulate the containment barriers from the high debris bed temperatures expected during the experiment. A liquid tin thermal bond between the double bottoms of the crucible provided a heat transfer path for downward cooling of the bed. Thermocouples

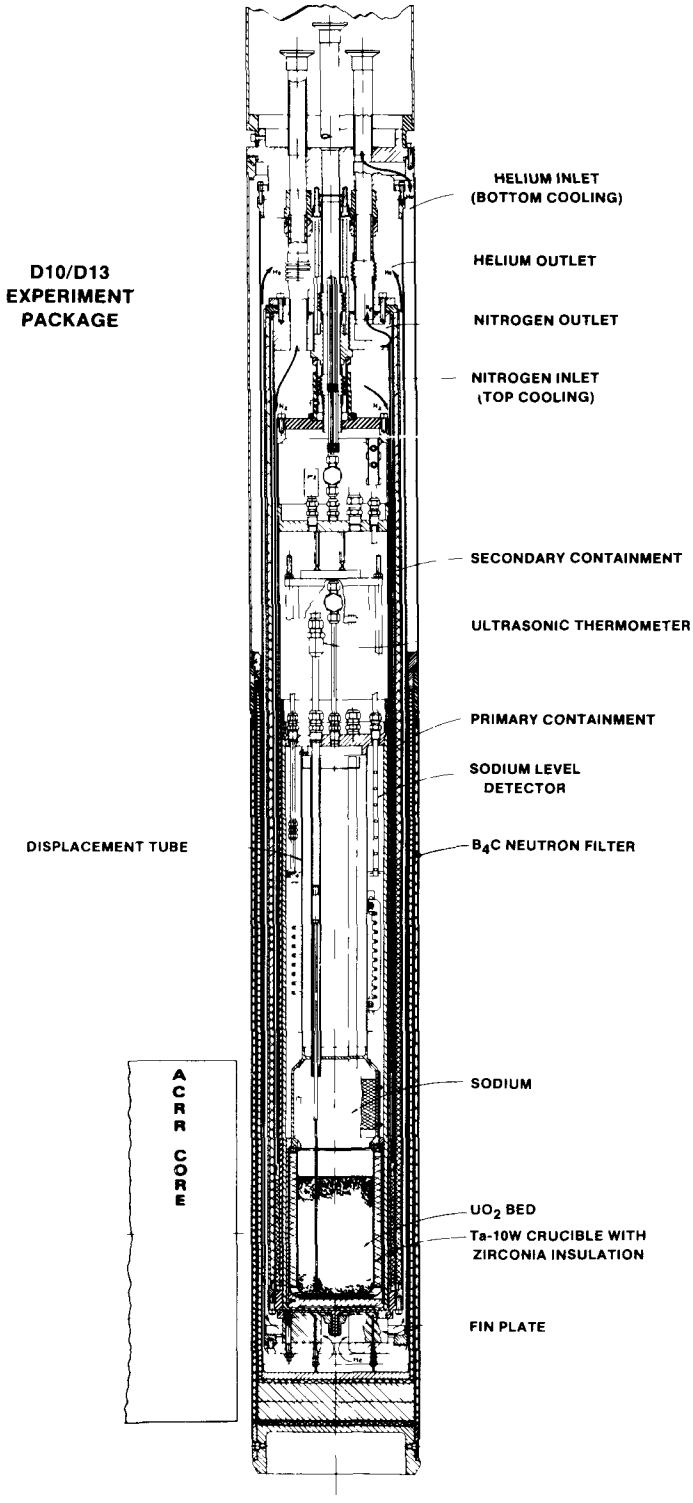

Figure 1. Experiment Section

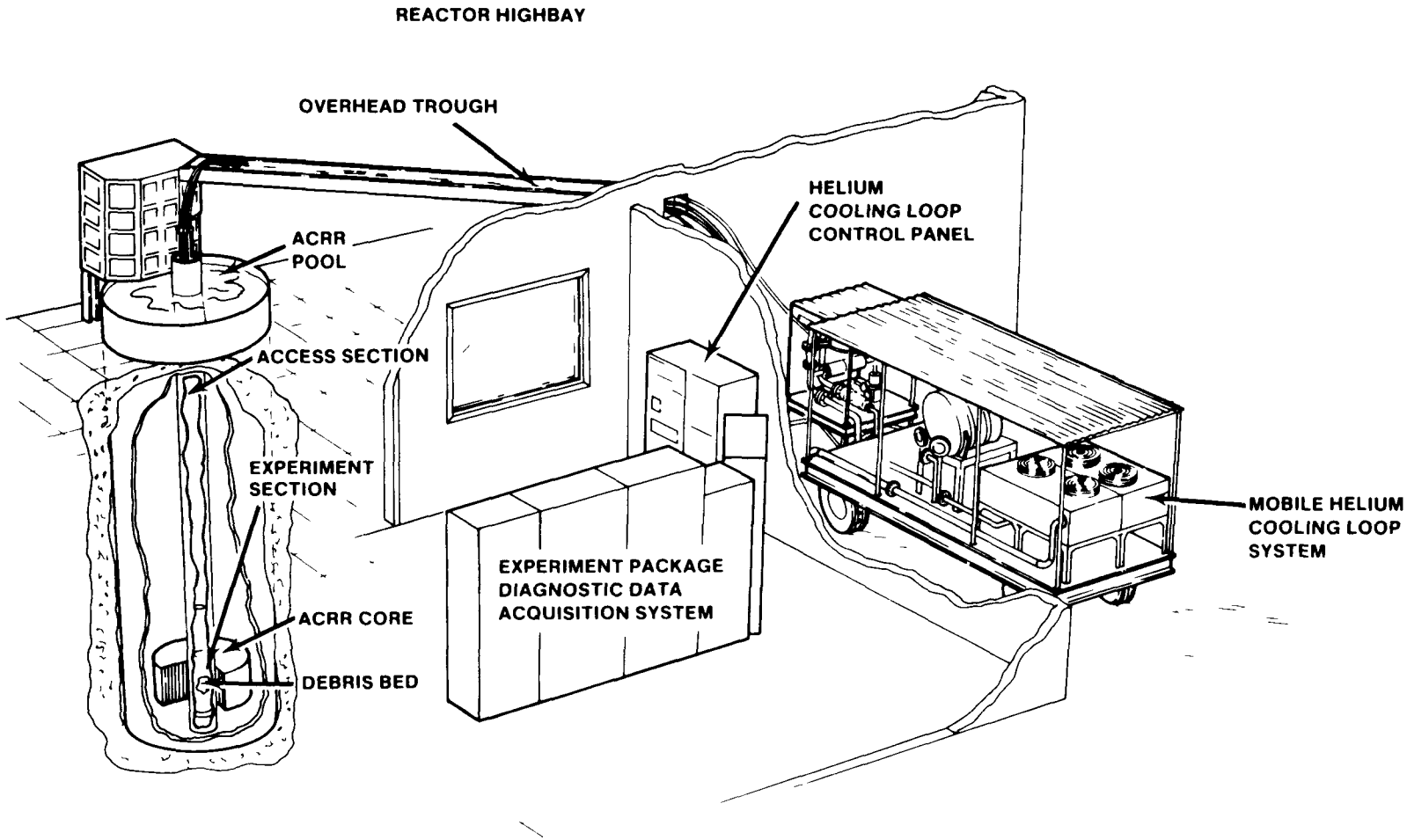

Figure 2. D13 Experiment Assembly Installed in the ACRR

were placed in the experiment so as to minimize perturbations, which would adversely affect the data, but in sufficient quantity to obtain the data necessary to characterize bed behavior. A primary radiological containment surrounded the crucible and held the sodium. A second containment surrounded the primary. Two independent gas cooling loops provided cooling for both the sodium pool overlying the bed and the bottom of the bed.

2.2.1 Instrumentation

2.2.1.1 High Temperature Thermocouples

Because of the experience they gained in fabricating a fuel centerline thermocouple capable of operating at 2200°C,[7] Hanford Engineering Development Laboratory (HEDL) was contracted to fabricate sodium compatible thermocouples capable of operating at 2300°C. They were successful in producing thermocouple assemblies that were accurate to within +1 percent after operating for 50 hours at a maximum temperature of 2300°C and were later qualified for operation at a maximum temperature of 2400°C. Using these thermocouples, we recorded valid data in the D10 experiment to a maximum measured temperature of 2240°C.[6] Development of these thermocouples was reported by HEDL in Reference 8.

The rhenium sheathed thermocouples consisted of tungsten 5/26 rhenium thermoelement wire with high purity hafnia insulators manufactured by National Beryllia Corporation. The rhenium sheaths provided a hermetic boundary for the thermocouples at high temperatures and in a sodium vapor environment. Ultramet fabricated the sheaths using the CVD process with a wall thickness of 0.25 mm. Details of the thermocouple sheath, which extended into the debris bed and the thermoelement junction, are shown in Figure 3. The rhenium sheath of each thermocouple was joined to a steel sheathed extension cable that fed the thermoelement wire out of the experiment. The thermocouples were incorporated into assemblies of four, which were brazed into feedthroughs to maintain the required containment barriers. These assemblies were required to operate in an environment of sodium liquid and vapor and, therefore, were fabricated from SS304, nickel alloys, and Nicrobraze.

2.2.1.2 Experiment Instrumentation Locations

The bed was instrumented with 14 high-temperature rhenium sheathed W/Re (C-type) thermocouples and 6 1.5-mm diameter steel sheathed K-type thermocouples. Additional steel sheathed K-type thermocouples were used to measure sodium temperature, the temperatures of a 10-mm thick SS304 heat

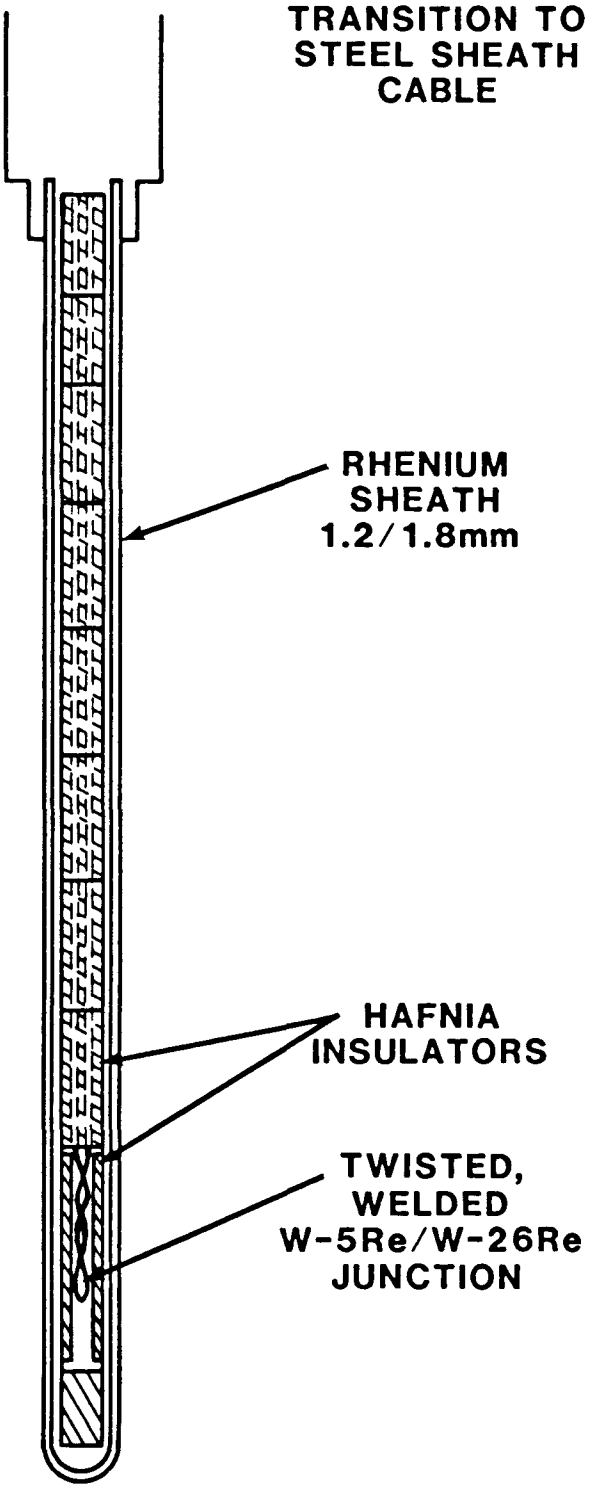

Figure 3. C-Type Thermocouple Detail

flux plate located below the crucible, and the temperatures of the containment structure, which were limited to 700°C as part of the experiment safety requirements.

A summary of instrumentation locations in the experiment is contained in Figures 4 and 5 and in Table 1. Estimated position error for the thermocouples is ±2 mm. The C-type thermocouple error is largely due to the fact that the twisted wire junction was 5 mm long. This positional error has a potentially large influence on the interpretation of data in regions of steep temperature gradients.

The high-temperature thermocouples penetrated the bed from above and were not bent because of the hard fired hafnia insulation. The K-type thermocouples were routed along the crucible wall and were bent into the bed at a constant elevation to the position indicated.

2.2.1.3 Pressure Transducers

Two Kaman Sciences KP-1911 pressure transducers were installed in both the primary and secondary containment vessels. These transducers performed a safety function of detecting leakage in either of the two containment barriers. Because of the thermal gradients imposed on the transducers during the experiment, the accuracy of the transducers was about ±0.15 bar.

2.2.1.4 Data Acquisition System

The thermocouple data were normally sampled at 3-second intervals by an HP9845 minicomputer with a capability for faster sampling rates at selected intervals. The data were stored on disk by the HP9845 and were transmitted to an HP1000 for backup data storage and data display during the experiment.

2.2.2 Bed Characteristics

The D13 debris bed consisted of 7,341 g of fully enriched UO_2 particles with an approximately lognormal distribution ranging from 38 to 4000 microns. The effective particle diameter, calculated by the Fair-Hatch formula, is 173 microns. The UO_2, with an average density of 10.26 g/cm^3, formed a bed 16 cm high with a total volume of 1280 cm^3, giving a calculated average open porosity of 43.5 percent. The particles were placed in the crucible in 24 layers to provide particle stratification by size, with the largest particles on the bottom. The makeup of these layers is shown in Table 2.

The particles were prepared by the Los Alamos National Laboratory by reduction of UO_3 in flowing hydrogen for 1 hour at 650°C followed by sintering for 1 hour in flowing

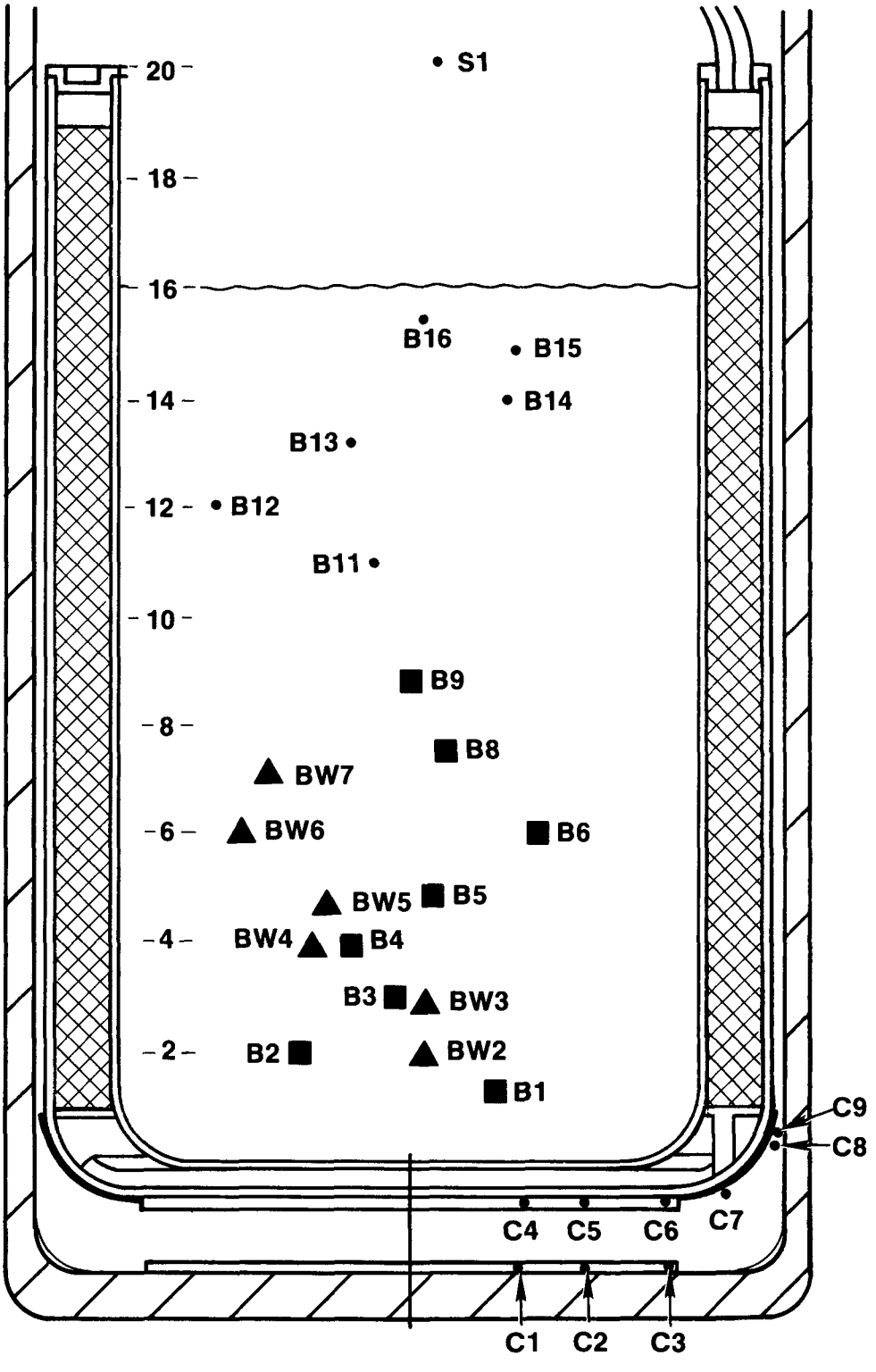

Figure 4. Thermocouple Layout

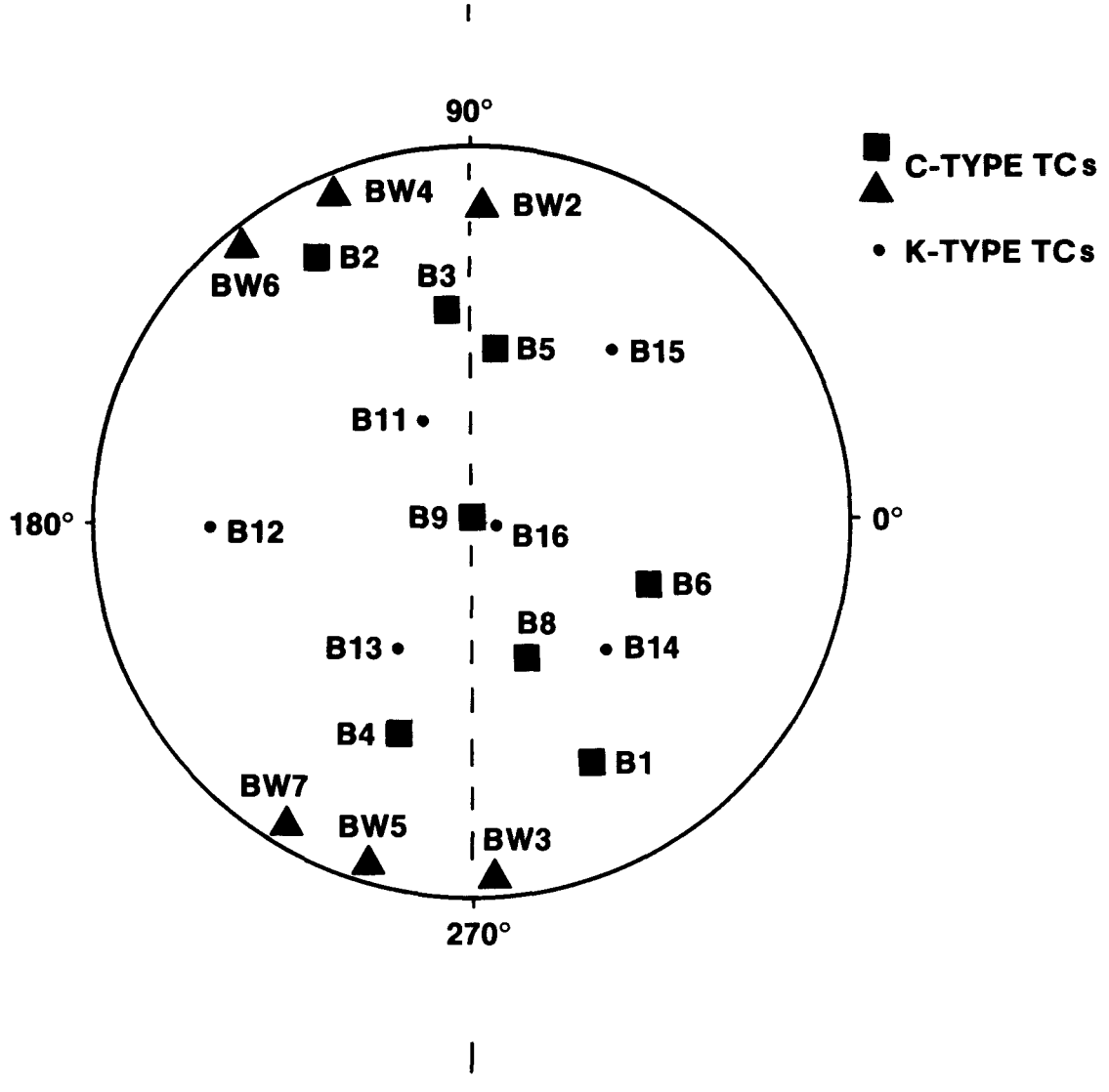

Figure 5. Thermocouple Layout

Table 1

Thermocouple Locations

Thermocouple	Radius (mm)	Z (mm)	θ (°)
B1	37	13	295
B2	41	20	120
B3	29	30	95
B4	30	40	250
B5	24	49	80
B6	25	60	340
B8	20	75	290
B9	0	88	0
B11	15	109	115
B12	35	120	180
B13	20	131	240
B14	25	139	315
B15	30	148	50
B16	3	154	350
BW2	40-45	20	85
BW3	51	29	275
BW4	51	39	110
BW5	48	47	250
BW6	51	60	130
BW7	51	71	240
S1	5	200	10
S2	0	235	0
S3	60	530	-

Table 2

UO_2 Bed Loading

Layer	Layer Wt (g)	Thick-ness (mm)	Size Ranges (μm)													
			2800-4000 μm	2000-2800	1400-2000	1000-1400	710-1000	500-710	355-500	250-355	180-250	125-180	90-125	63-90	45-63	38-45 μm
1	264	8	212	52												
2	260	4	53	207												
3	205	3		86	119											
4	238	5			239											
5	263	4			119	144										
6	286	5				287										
7	312	6				143	170									
8	338	7					338									
9	360	8					169	191								
10	382	7						382								
11	387	8						191	196							
12	393	9							393							
13	394	8							196	198						
14	396	8								397						
15	369	5								198	171					
16	342	11									342					
17	338	7									171	167				
18	334	5										334				
19	292	8										167	125			
20	249	7											250			
21	229	6											125	105		
22	209	5												209		
23	244	6												105	140	
24	257	9.5													139	118
	7341g	159.5 mm	265 g	345 g	477 g	573 g	677 g	763 g	785 g	793 g	684 g	660 g	499 g	419 g	279 g	118 g

helium and water vapor to obtain a ceramic-type UO_2 stable in air. The UO_2 was then pressed, crushed, sieve sized, and fired in hydrogen at 1800°C for 24 hours. The fired particles were further crushed and sieve sized to obtain the final particle distribution. The tendency for this UO_2 to adsorb water vapor was investigated at the Sandia National Laboratories (SNL).[9] After 5 days in an 85 percent humidity environment, the UO_2 adsorbed approximately 0.015 percent water by weight. This water was easily desorbed within a few hours by heating to 100°C in vacuum.

As part of the experiment assembly in preparation for sodium filling, the primary containment, including the UO_2 debris, was baked out under vacuum for several hours. This bakeout was initiated by evacuating the sealed containment and leaving it connected to a cold trapped diffusion pump for a period of 16 hours at room temperature. It was then backfilled with argon and heated to 300°C in a period of 5 hours. Twice during the heatup the containment was evacuated and purged with argon. The containment was then evacuated with a measured pressure at the inlet to the diffusion pump of 1×10^{-5} Torr. After 4 hours at a temperature of 300°C, the pump inlet pressure had dropped to 2.2×10^{-6} Torr. At this point the sodium filling procedure was altered from that of the previous debris bed experiments.

While the containment was still evacuated, a small amount of sodium was introduced into the containment. This was done to try to get sodium into the small spaces in the heat flux plate below the crucible. Then the containment was backfilled with less than 0.001 bar helium prior to filling the remaining sodium. The small amount of helium was intended to provide a small amount of noncondensable gas on the debris so that a sodium superheat would be avoided during the initial heatup and approach to boiling during the experiment.

Following sodium filling the containment was X-rayed. Photographs of these X-rays showing the UO_2 bed in the crucible and the primary containment are shown in Figures 6 through 8. During the loading, the bed height was 159.5 mm, and after sodium filling, it was 155 mm. The bed sustained some settling during final assembly between the bed loading and sodium filling. The preexperiment radiographs indicated a top bed surface level variation of approximately 10 mm, which was the thickness of the top layer.

2.2.3 Experiment Neutronics

To determine the expected power profiles in the UO_2 debris, two-dimensional neutron transport calculations were performed with the TWOTRAN code.[10] For these calculations the bed was defined by 8 equally spaced radial zones and 10

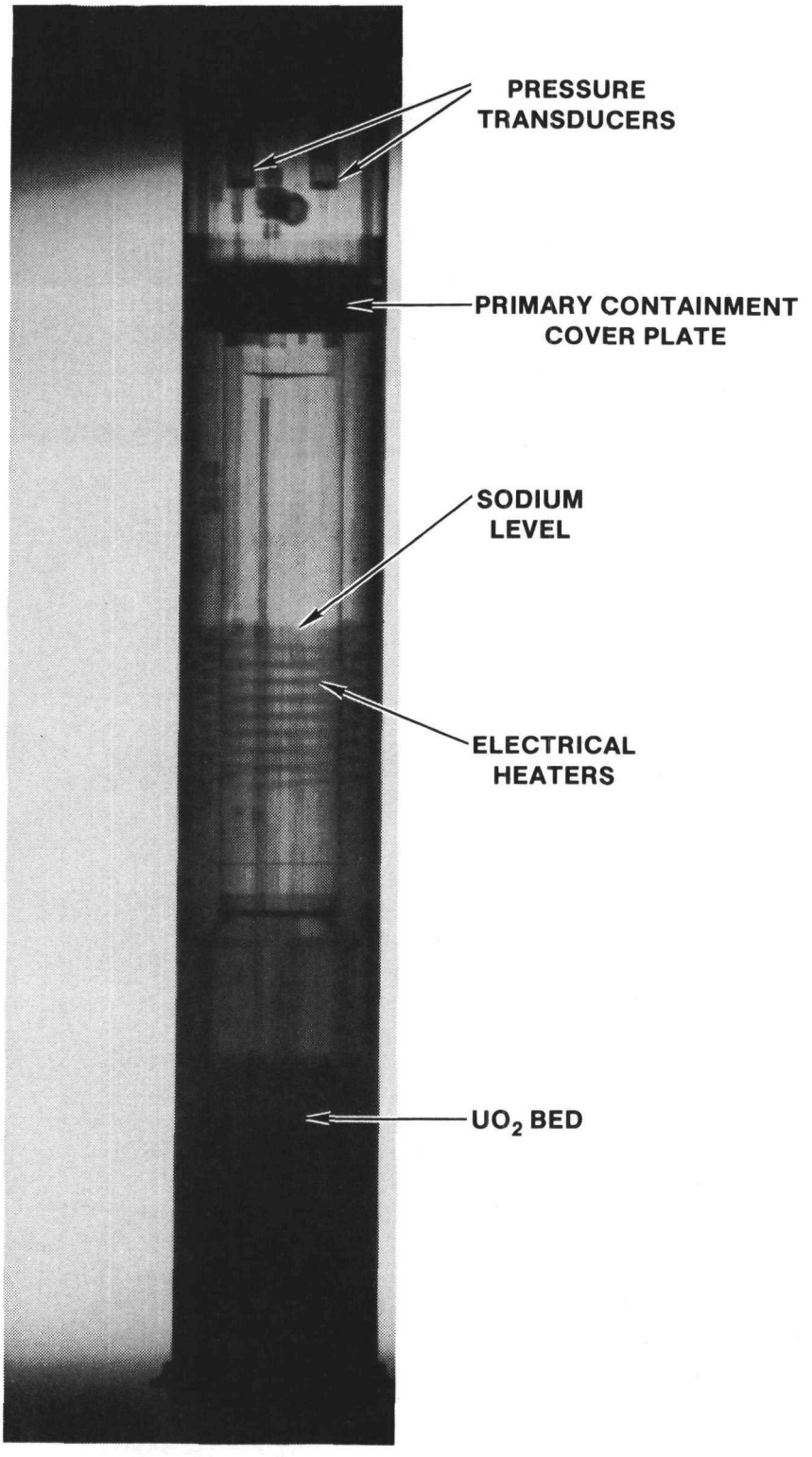

Figure 6. Pretest X-Ray of Primary Containment

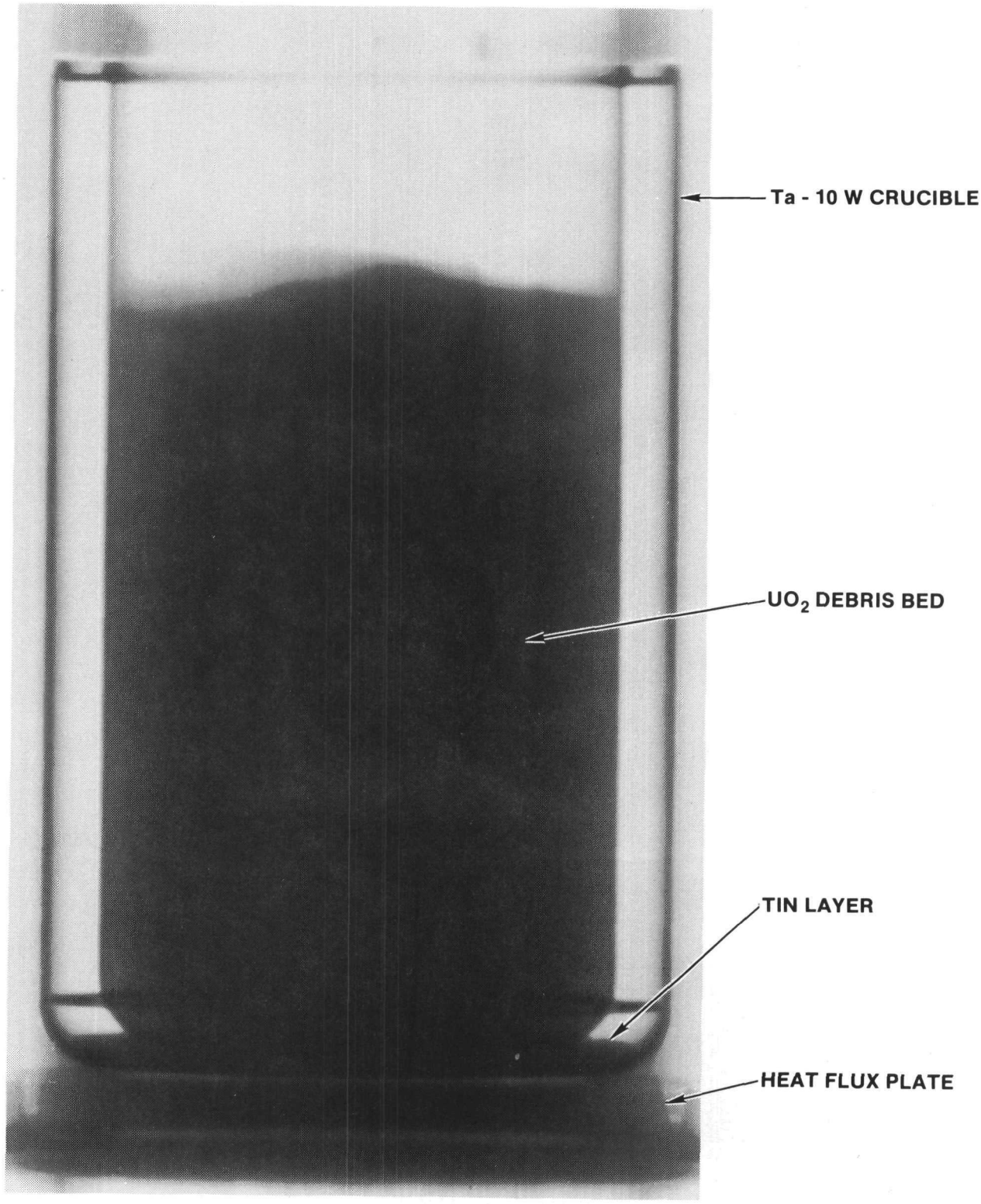

Figure 7. Pretest X-Ray of UO_2 Bed in Crucible (0°)

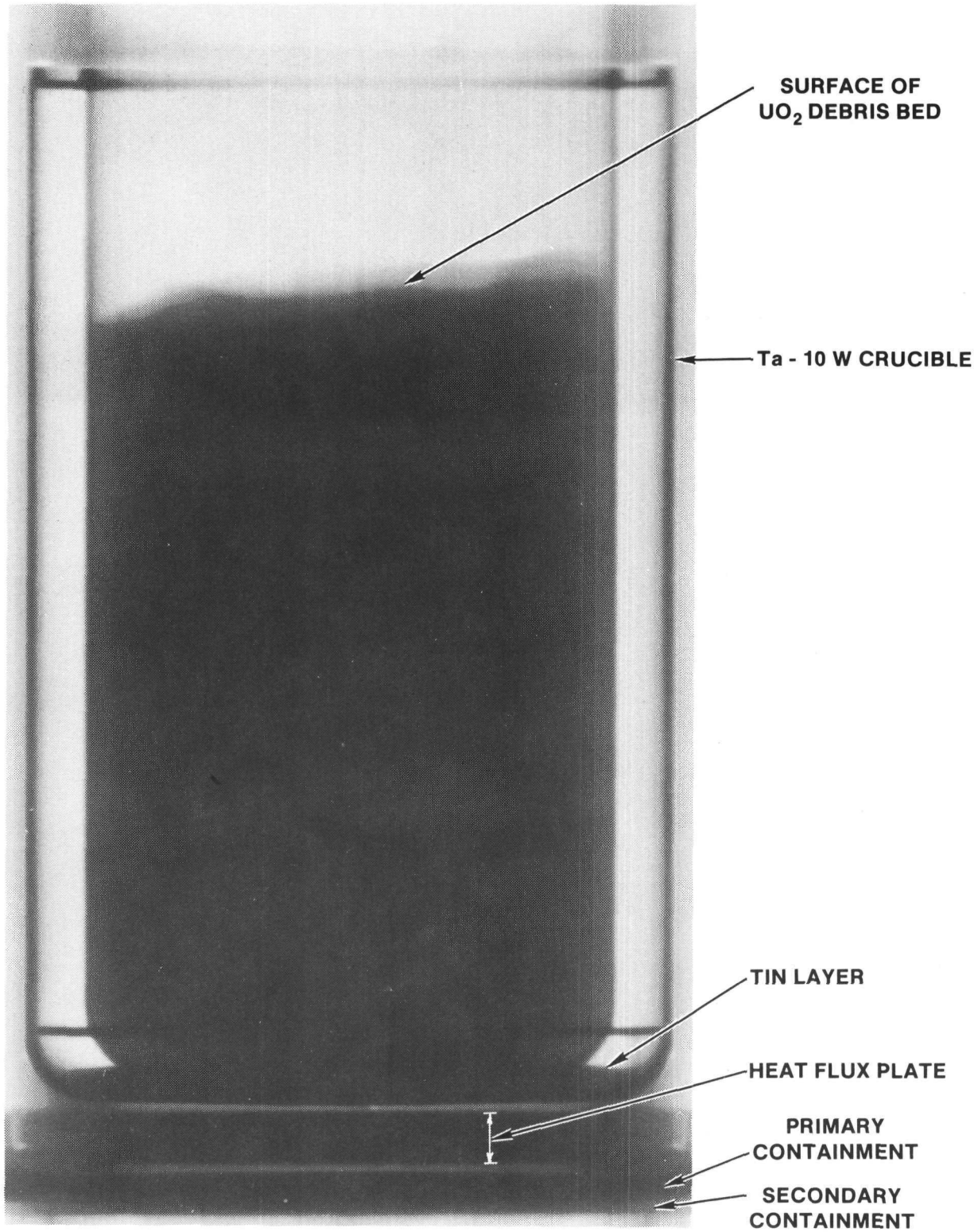

Figure 8. Pretest X-Ray of UO_2 Bed in Crucible (90°)

axial zones, and a 9-group cross-section set tailored to the fast neutron spectrum, which exists in debris bed experiments, was used. Power peaking occurs at the radial boundary of the bed and at the top of the bed, with a maximum peak to average power ratio of about 1.1.

3. EXPERIMENTAL PROCEDURES AND RESULTS

The operating procedures to most efficiently obtain the desired data were proposed in June 1984 and were subsequently reviewed by program sponsors and SNL project staff prior to operation of the experiment. These procedures included conduction/convection investigations, two-phase heat removal, and incipient dryout all at various rates of downward heat removal. Extended dryout investigations would be made with a series of small power steps allowing for steady state at each step and with high subcooling and a low bottom temperature initially followed by decreasing bottom cooling. Then the sodium subcooling would be decreased and the dryout investigations continued. Finally, channeling investigations would be made using power ramps of about 0.1 W/g/min rather than the fast ramps used during D10 to avoid a bed disturbance. The high temperature extended dryout investigations would be performed with a fast power ramp of about 1.0 W/g to achieve maximum power within 20 s. Appendix A is a copy of these procedures.

3.1 Conduction/Convection Results

The experiment was started on March 11, 1985, by melting the sodium using the internal electrical heaters. After reaching a sodium temperature of 250°C, nuclear heating was initiated. The first control run was established at a sodium temperature of 350°C and an ACRR power of 90 kW to establish a reference temperature profile against which to make comparisons later in the experiment. A power calibration was then conducted by increasing ACRR power from 90 to 300 kW for a period of 2 min and observing the temperature rise. This calibration gave a power ratio of 1.86 W/g-MW_{ACRR}. From this point onward, recorded ACRR power levels were used to infer instantaneous debris bed power. The sodium temperature was then increased to 600°C and power was increased to achieve UO_2 temperatures of about 800°C which were maintained for a period of 1.5 hours to insure wetting of the UO_2 by the sodium. Various subcooled temperature profiles were then established in the bed at different sodium temperatures and rates of downward cooling. Instead of using the bottom (helium) flow rate as the controlling parameter to vary the rate of downward cooling as was done in the D10 experiment, the temperature below the heat flux plate (C1/C2) was used. The wide range of helium flow rates could be utilized to overcome the thermal inertia of the bottom structures and change the temperature of the heat flux plate much more quickly. The temperature at the bottom of the bed is related to C1/C2 by the heat flux through the stainless steel heat flux plate. The experimental conditions during the conduction/convection investigations are summarized in

Table 3. The $Z_{a,c}$ column refers to the location of the adiabatic plane in the bed, calculated from temperature measurements in the bed.[11]

Temperature profiles during these first investigations were compared with two-dimensional calculations made using the Kampf-Karsten conductivity for the bed. The calculations were consistent with the observed data, indicating that the assumed conductivity was appropriate.

Table 3

Conduction Investigations (March 11-12)

Time	Event	Bed Power (W/g)	C1/C2 (°C)	$Z_{a,c}$ (mm)	Sodium Temp (°C)	Max Bed Temp (°C)
1608	CR1	0.17	451/448	56	350	552
1610	PC1	0.56	459/456		350	673
1806	CR2	0.20	670/664	65	600	835
1856	CR3	0.20	488/487	76	601	751
1936	CR4	0.20	341/341	99	602	697
2007	CR5	0.31	335/336	87	601	807
2103	CR6	0.17	347/349	65	354	507
2316	CR7	0.19	521/517	52	350	624
2318	PC2	0.54	527/523		354	735
1009	CR8	0.49	301/302		500	840
1154	CR9	0.39	566/555		400	799
1822	CR10	0.41	500/502		540	811
1823	PC3	1.07	503/506		552	913

CR = Control or Conduction Run

PC = Power Calibration

3.2 Two-Phase Heat Removal

Following the second power calibration at a sodium temperature of 350°C, power was slowly increased to initiate boiling in the bed. The onset of boiling is detected by noting when the temperature difference between two levels in

the bed begins to decrease in response to a power increase, which results from the improved effective thermal conductivity from two-phase heat transfer. The saturation temperature is a function of the location in the bed because of varying capillary pressure. This type of boiling behavior was noted in D5, D7, and D9. However, temperatures in the bed increased above the expected saturation temperature without initiation of boiling.

At a power of 0.42 W/g, bed temperatures dropped rapidly from a maximum of 928°C to ~850°C. This indicated that a superheat flashing event of 78°C had occurred. Following this event, boiling was indicated on thermocouples B1 to B6 (from 13 mm to 60 mm). The superheat flashing event occurred prior to any boiling in the bed, indicating that there had been very little trapped gas in the bed to provide nucleation sites, in spite of the addition of helium to the primary containment during the sodium filling procedure.

The bed was allowed to stabilize and then power was reduced in several small steps to reduce the size of the boiling zone. At 0.36 W/g, the boiling zone was still 30 cm thick.

Power was then increased in steps until incipient dryout was observed on B6 (at an elevation of 60 mm) at a power 0.94 W/g. Power was increased to extend the size of the dry zone. At a power level of 1.28 W/g, dryout occurred at B5 and at B4. As power was increased to 1.45 W/g and 1.64 W/g, thermocouples BW5 and BW3 on one side of the crucible wall indicated that the dry zone had increased in extent to their location. At a power level of 1.81 W/g, B1 indicated dryout. Thermocouple B3 indicated a dry zone very briefly at this power level, but it did not stabilize. Thermocouple B2 never indicated a stable dry zone. The dryout was quenched when the sodium temperature reached 600°C and the bottom containment temperature reached 700°C.

In an attempt to achieve a stable dryout extending across the bed, without excessively heating the sodium or the primary containment, power steps were made from ~0.37 W/g to ~1.80 W/g. A stable dry zone existing across the bed is desirable to prevent shunting of heat from below the dry zone, past the dry zone, and to the region above the dry zone. A partition of upward and downward cooling cannot be determined if this occurs. In the first two attempts, dryout did occur at several thermocouples in the bed, but the containment temperature also rose rapidly. In dryout 4, the containment temperature remained at an acceptable temperature for over 5 min, allowing the dry zone to extend again to thermocouples B3, B4, B5, and B6 and on the wall thermocouples BW3 and BW5. Again, thermocouples B1, B2, B8, and B9 showed temperatures indicating dry zones, but these zones were unstable and would quench periodically.

For the stratified D13 debris bed, packed bed dryout had been expected to occur at powers only slightly above that required for boiling, as seen in the previous stratified debris bed experiments (D6, D7, and D9).[3,4,5] However, the incipient dryout power of the D13 bed following the superheat flashing event was much higher than the power required for boiling. Also, even at twice the incipient dryout power, the dry zone did not extend across the entire bed. Instead, regions of the bed would become dry and then quench periodically. This indicates that the superheat flashing event disrupted the bed stratification and induced the formation of channels in the bed. Since one of the major objectives of the D13 experiment had been to study packed bed dryout, several attempts were made to reestablish a packed bed condition.

Following dryout 5, the sodium temperature was lowered to 500°C and the bed was subcooled 35°C in an attempt to pack the bed. Power was then increased and a 27°C superheat flash occurred prior to the initiation of boiling. The bottom cooling was increased to lower the bed bottom temperature and raise the adiabatic plane to raise the boiling zone (and reduce the size to <2 cm) to a higher level. With the smaller particles assumed to exist at this higher level, perhaps a new dryout power could be measured. Power was increased in small steps to 1.4 W/g and dryout was not observed. This indicated that a packed bed had not been reestablished.

Another attempt was made to reestablish a packed bed by allowing the bed to subcool slightly. An assumption was that if liquid filled all the vapor regions, perhaps the channels would collapse. The bed was subcooled 40°C, and when power was increased a 47°C superheat flash occurred. Power was increased to 1 W/g with no dryout observed. Power was stepped to 1.6 W/g and, when dryout was still not observed, returned to 0.4 W/g to again subcool the bed.

A final attempt was made to reestablish a packed bed by disrupting the particles with a superheat flash. The bed was subcooled significantly and the downward cooling decreased. This would increase the volume of the bed involved in the superheat disturbance. Immediately after the flash, power would be decreased to allow the UO_2 particles to hopefully resettle in a packed state.

The bed was subcooled 110°C, and a superheat flash of 79°C occurred when power was increased from 0.4 W/g to 0.7 W/g. Power was first reduced back to 0.4 W/g and then increased to 1.05 W/g with no dryout observed.

It was then decided to continue with dryout measurements with the bed in a disrupted state. Dryout 6 occurred with a sodium temperature of ~600°C and C1/C2 temperatures of 500°/470°C at a power of 2.57 W/g. This dryout was very unstable.

Dryout 7 occurred with the sodium temperature increasing from 500°C to 600°C and C1/C2 temperatures at 499°/474°C. The bed power was 2.58 W/g and dryout was stable on thermocouples B4, BW3, and BW5.

Dryout 8 (Figure 9) occurred with a sodium temperature of ~600°C and higher C1/C2 temperatures of 578°/564°C. The dryout power was 2.54 W/g and was stable on thermocouples B4, B6, BW3, BW5, and BW6, indicating that the dry zone extended across the bed.

The last dryout of this session, dryout 9 (Figure 10), was achieved by stepping the power from 0.74 to 3.27 W/g and then reducing the power in two steps to 2.21 W/g, where temperatures were somewhat stable. The sodium temperature started at 400°C and rapidly rose to ~600°C. Heat flux plate temperatures (C1/C2) stabilized at ~575°/555°C. At the initial power of 3.27 W/g the dry zone was 3 cm thick and occurred at thermocouples B3, B4, and B6, and wall thermocouples BW3, BW5, and BW6. When the power was reduced to 2.61 W/g, dryout was no longer indicated on B3, but still extended across the bed. The power was further reduced to 2.21 W/g and held at this power. Initially, dryout was indicated on bed thermocouples B4 and B6 and wall thermocouples BW3 and BW5. As this power level was maintained, only thermocouples B6 (60 mm) and BW3 (28.5 mm) remained in the dry zone, indicating a very nonuniform dry zone. The dryouts and flashing events are summarized in Tables 4 and 5, respectively.

Following a final control run and power calibration, the experiment was shut down for discussions and determination of procedures for the second session.

3.3 Session 2 Operations

Since a major objective of the D13 experiment was to measure packed bed dryouts, the first part of the second session was again devoted to reestablishing a packed bed. The second session was started March 14, 1985, by using the electrical heaters to melt the sodium, followed by nuclear heating. A control run was established with a sodium temperature of 500°C and a bottom temperature (C1/C2) of ~500°C. A power calibration was conducted by raising ACRR power from 120 to 300 kW. The bed characteristics were similar to those at shutdown on March 12.

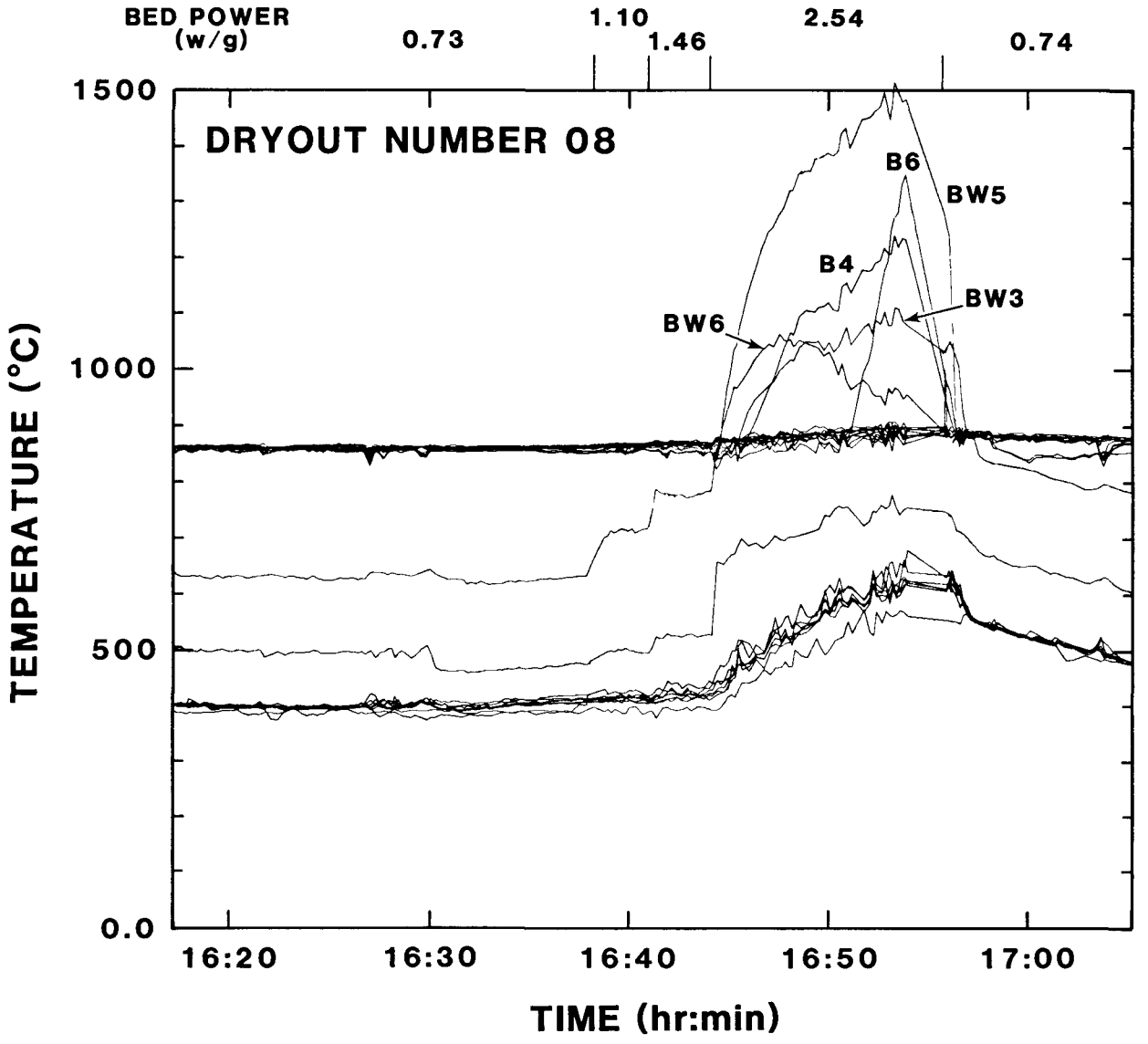

Figure 9. Dryout 8 (March 12)

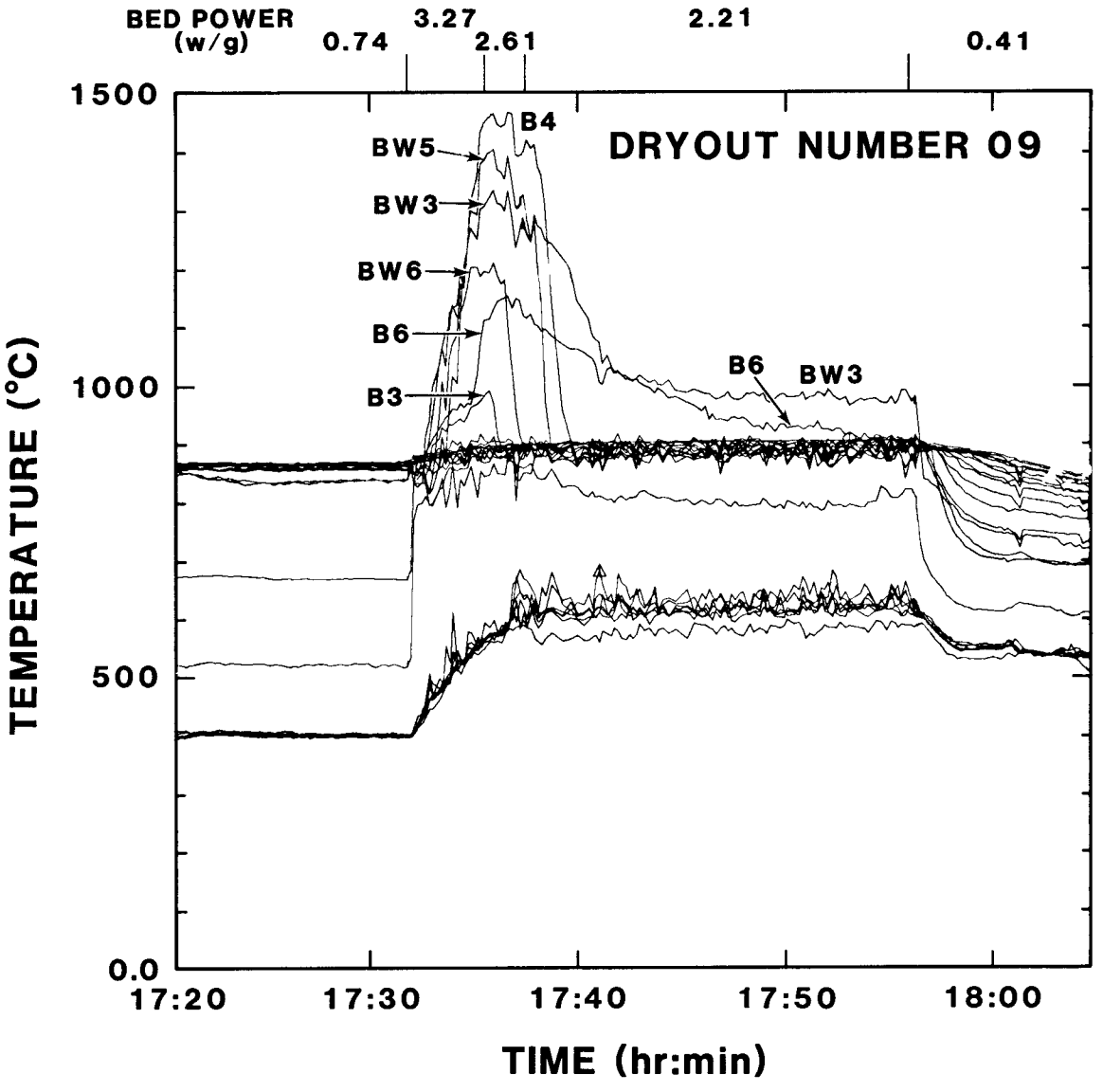

Figure 10. Dryout 9 (March 12)

Table 4

Channeled Bed Dryout (March 12)

Time	Event	Bed Power (W/g)	C1/C2 (°C)	Sodium Temp. (°C)	Max. Measured Bed Temp. (°C)
0454	DO1	0.94	698/677	350 (initially)	1279
0602	DO2	1.80	700/690	598	922
0611	DO3	1.78	681/681	615	929
0620	DO4	1.78	680/661	607	1209
0644	DO5	2.35	662/631	557	1342
1505	DO6	2.57	500/470	630	940
1555	DO7	2.58	499/474	570	1282
1647	DO8	2.54	578/564	560	1517
1733	DO9	2.21	575/555	615	1470*

*At initial bed power of 3.27 W/g

Table 5

Superheat Flashing Events (March 12)

Time	Event	Bed Power (W/g)	Subcooled (°C)	Superheat (°C)	Na Temp. (°C)
0126	F1	0.42		78	348
0701	F2	0.79	18?	29	500
1013	F3	0.71	48?	49	500
1200	F4	0.67	90	77	400

Immediately following the power calibration the reactor was shut down. With the bed and sodium at temperatures in excess of 400°C, an attempt was made to mechanically settle the particles. The entire experiment assembly was raised approximately 1 in with the ACRR crane and then set back down. This created a firm tamping of the experiment contents and was repeated several times.

The reactor was restarted and the previous control run and power calibration were repeated. Upon ACRR startup, it was noted that the reactivity of the experiment increased slightly, indicating a possible settling of the UO_2 particles. Sodium temperature and bottom temperature (C1/C2) were lowered to 350°C for the next control run. The sodium temperature was held constant for the next power calibration. The control runs and power calibrations are summarized in Table 6.

Table 6

Conduction Investigations (March 14)

Time	Event	Bed Power (W/g)	C1/C2 (°C)	Sodium Temp. (°C)	Max. Bed Temp. (°C)
1004	CR11	0.22	463/465	509	639
1005	PC4	0.55	473/475	514	727
1046	CR12	0	428/431	441	440
1114	CR13	0.23	461/463	506	643
1115	PC5	0.55	467/469	503	739
1216	CR14	0.22	349/348	348	496
1222	PC6	0.55	420/419	349	653
1935	CR15	0.27			
1936	PC7	0.55			

CR = Control or Conduction Run

PC = Power Calibration

With sodium temperature held at 350°C, power was increased slowly to approach boiling. A small (15°) flash occurred prior to the initiation of boiling. Power was increased in steps to 1.64 W/g to search for incipient dryout. Dryout was not observed at this power level, indicating that the bed had not repacked and was still channeled. Power was lowered to 0.74 W/g and the high-temperature investigations were started.

The sodium temperature was increased to ~650°C and the bottom (C1/C2) temperature to ~500°C and allowed to stabilize. For each subsequent dryout, the nitrogen and helium (downward) cooling were increased to the maximum and power stepped to ~3.4 W/g. Power was then decreased in several steps to try to stabilize the dry zone. This flashing event and dryouts are summarized in Tables 7 and 8, respectively. Measured bed temperatures in excess of 1800°C were maintained for a total of 1.25 hours during dryouts 11, 12, and 13. A peak measured temperature of 2440°C was measured during dryout 12.

Table 7

Superheat Flashing Event (March 14)

Time	Event	Bed Power (W/g)	Subcooled (°C)	Superheat (°C)	Sodium Temp. (°C)
1510	F5	0.53	-	15	351

Table 8

High-Temperature Dryout Investigations (March 14)

Time	Event	Initial Bed Power (W/g)	Final Bed Power (W/g)	C1/C2 (°C)	Approx. Sodium Temp. (°C)	Max. Measured Bed Temp. (°C)
1655	DO10	0.74	3.45	509/484	675	992
1711	DO11	0.74	3.48	455/450	600	2220
1800	DO12	0.74	3.43	500/450	575	2440
1830	DO13	0.05	3.27	550/535	600	2160

A distinction must be made between measured temperatures and actual debris temperatures. Three-dimensional heat transfer calculations were made prior to the experiment to determine the effect of instrumentation on bed temperatures and to relate measured temperatures to debris temperatures at locations not in proximity to the instrumentation.

These calculations indicated that the thermocouples would indicate temperatures less than the maximum bed temperatures due to heat transfer along the highly conductive sheath and due to the radial temperature gradient. For the thermocouples, located at radii of 25 and 30 mm, this gradient could result in a temperature drop of several hundred degrees.[12] For the purposes of discussion and for this preliminary interpretation of bed behavior, reference will be made to measured temperatures. Although additional three-dimensional calculations will be required to establish reliable estimates of the maximum debris temperatures, which were achieved in the experiment, the pretest calculations, which were accomplished, would indicate that debris temperatures in excess of 2700°C were achieved.

During dryout 11, shown in Figure 11, a dry zone was indicated at bed thermocouples B1, B2, B3, B4, B5, and B6 and wall thermocouples BW3, BW5, and BW6, indicating that the dry zone did extend across the bed. The dry zone did not remain stable at B1, B2, and B3 during this dryout. A peak measured temperature of 2160°C on B5 was recorded during dryout 11. The increasing temperature of B4 during the time at 2.55 W/g while B5, B6, BW3, and BW5 are relatively stable is indicative of a junction located below the location of the maximum temperature of the sheath. At high temperatures, the HfO_2 insulation becomes conductive and a shunting occurs, which causes an electromagnetic force (EMF) corresponding to the peak temperature to be measured. This shunting occurred gradually. The same behavior was noted during a high-temperature dryout in the D10 experiment.[6]

During dryout 12, shown in Figure 12, bed thermocouples B1, B3, B4, B5, and B6 and wall thermocouples BW3, BW5, and BW6 indicated a stable dry zone. Thermocouple B2 did not indicate a dry zone at any time. A peak temperature of 2440°C was measured on B5 during this dryout.

The final dryout, number 13 (Figure 13), showed a stable dry zone on thermocouples B2, B3, B4, B5, B6, BW2, BW3, BW5, and BW6. Occasional indications of a dry zone occurred on B1, B8, B9, B11, and BW4. Peak measured temperatures of 2080°C and 2160°C were recorded on B3 and B5, respectively.

Following a final control run and power calibration, the D13 experiment was shut down. All instrumentation, including

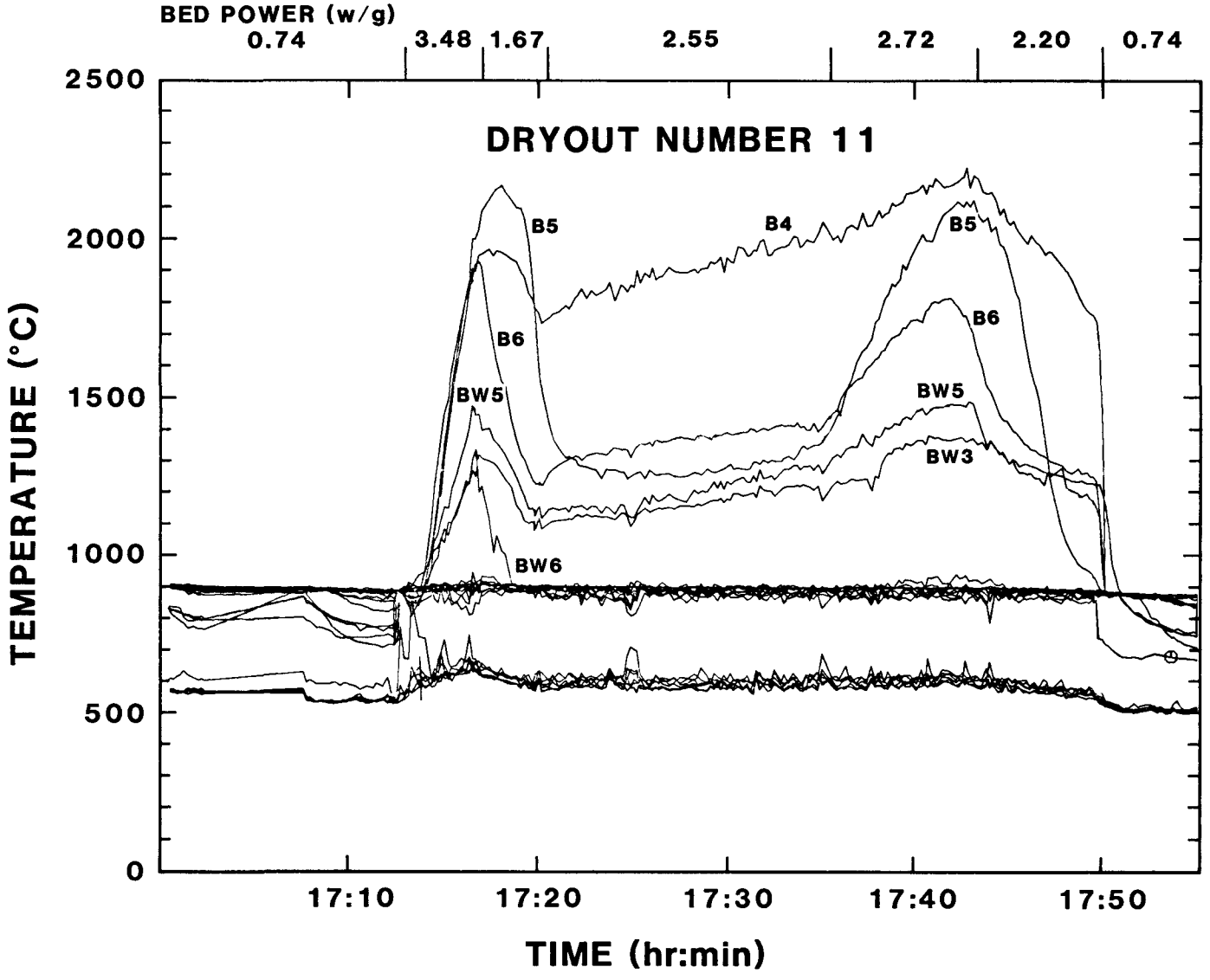

Figure 11. High-Temperature Dryout 11 (March 14)

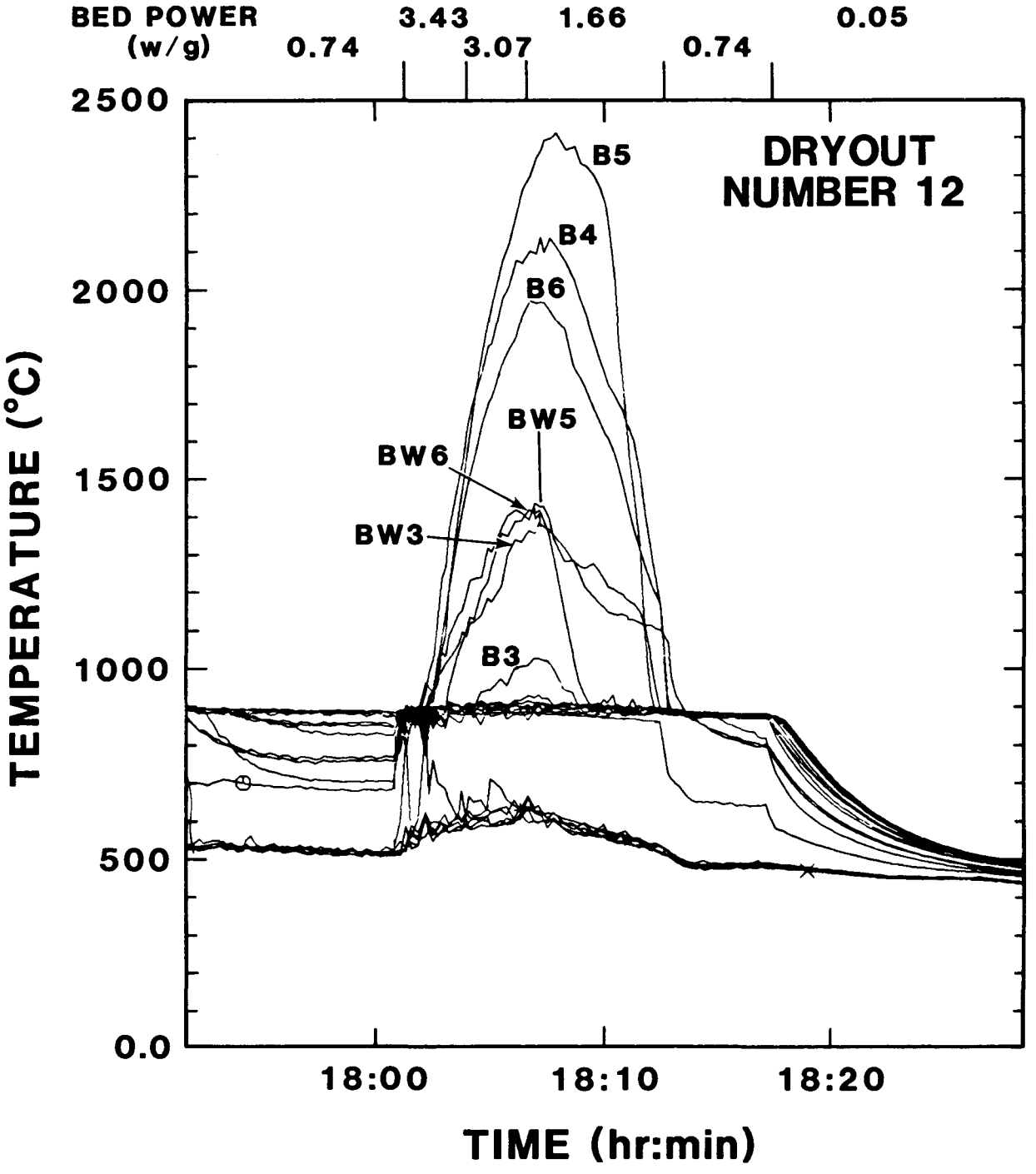

Figure 12. High-Temperature Dryout 12 (March 14)

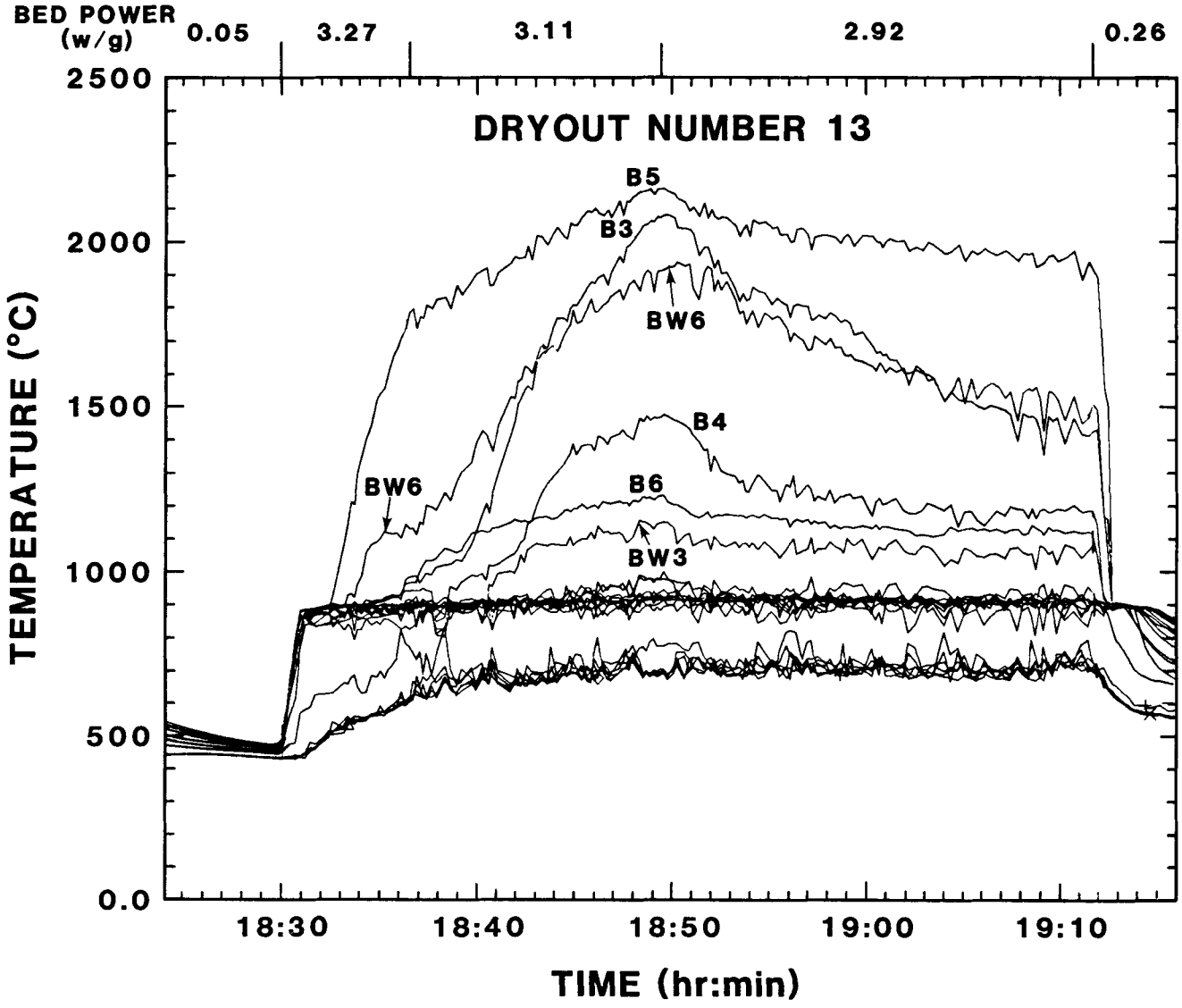

Figure 13. High-Temperature Dryout 13 (March 14)

the 14 high temperature W/Re thermocouples, were functioning properly at the conclusion of the experiment.

3.4 Bed Configuration

The configuration of the bed during the experiment, especially after the disruption event at the first onset of boiling, is critical to any analyses. This is important to establish the possible boundary conditions, which are the basis for such analyses. The X-rays of the bed taken after the experiment was completed, shown in Figures 14 and 15, indicate that the bed has an average height of about 130 mm with an 8 to 10 mm unevenness. This would indicate that the average height in the bed is about 25 mm shorter at the end than at the start of the experiment. The UO_2 ejected from the crucible is on the top surface of the basket, which holds the crucible, in a 5-mm-thick annulus. The UO_2 forms three dome-shaped piles in the annulus corresponding to the three openings between the support legs at the bottom of the displacement tube. These openings are located 14.4 to 16 cm above the top of the original 16-cm-tall debris bed. Although the new bed volume is known, the weight of the UO_2 remaining in the bed, or the weight of the UO_2 ejected from the bed is not known; therefore, an average bed porosity cannot be determined accurately.

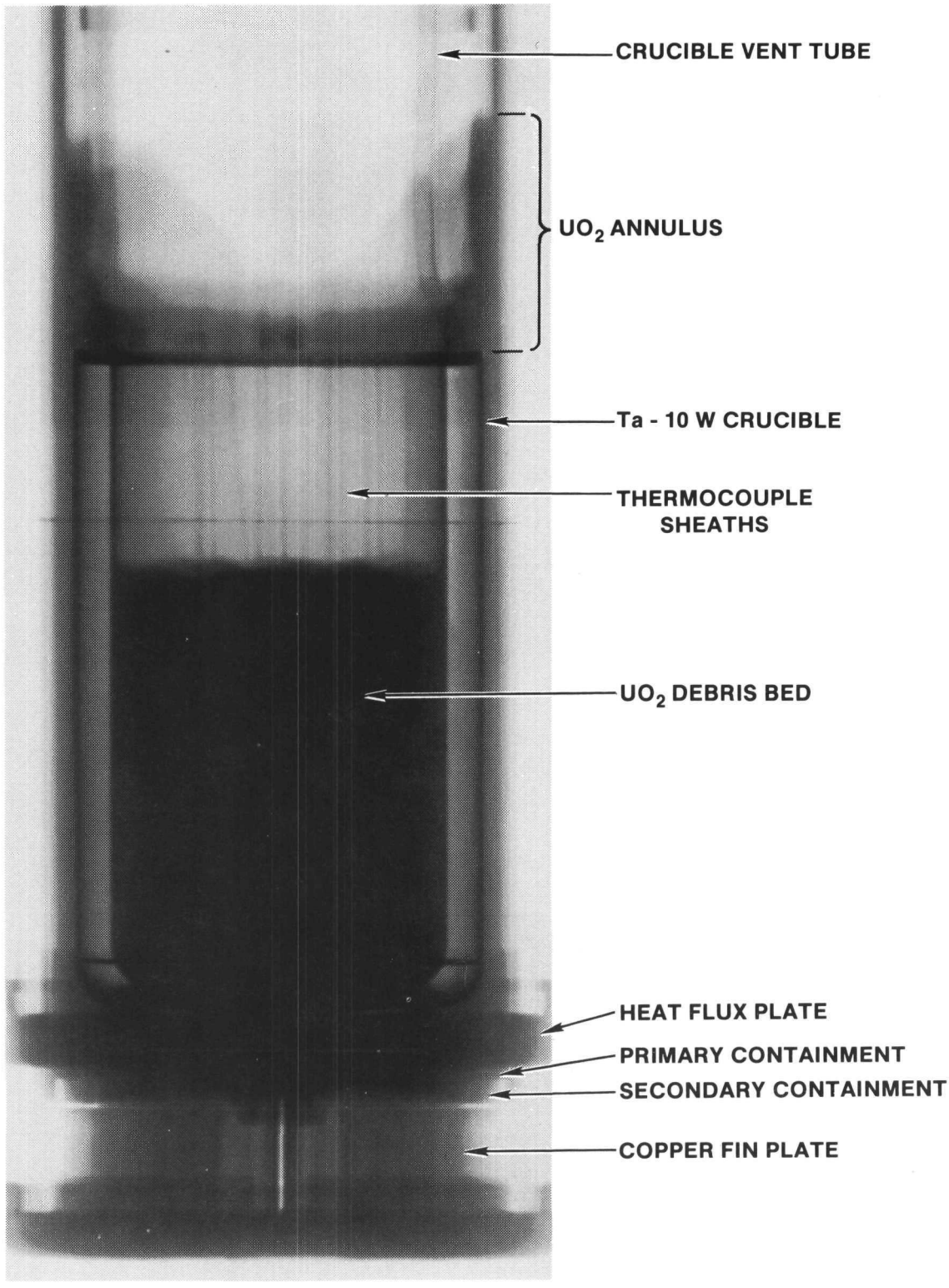

Figure 14. Posttest X-Ray of UO_2 Bed (0°)

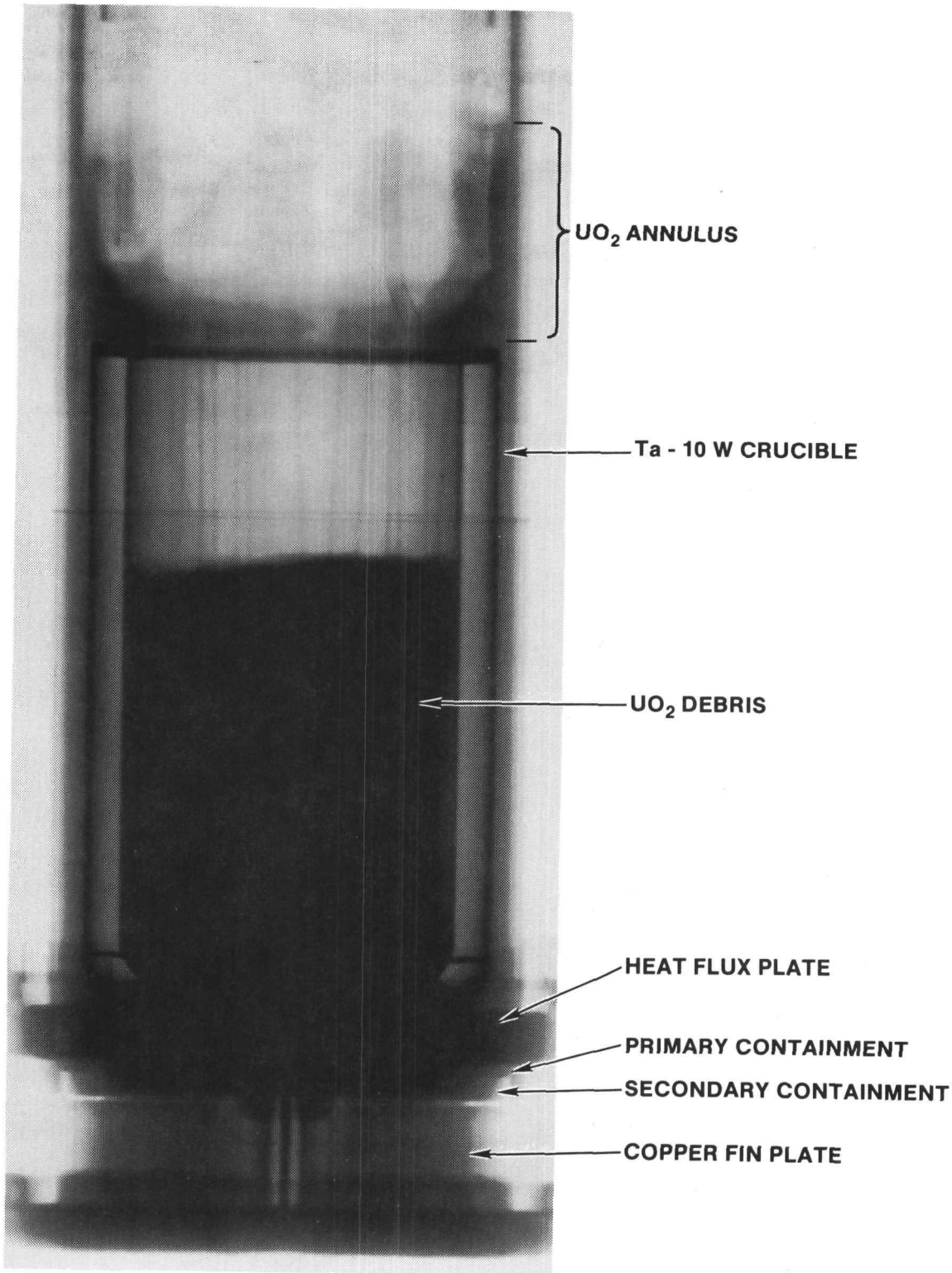

Figure 15. Posttest X-Ray of UO_2 Bed (90°)

4. ANALYSIS

In order to analyze the D13 experiment, certain approximations must be made concerning the D13 configuration. In particular, the layer depths measured during the fuel loading are not sufficiently precise. Uncertainties in individual depth yield uncertainties in the individual layer porosities. To approximate the geometry with sufficient precision to make realistic calculations, it was assumed that the porosity was constant throughout the bed and equal to the measured average porosity of 0.435. In consequence, the resulting layer thicknesses are directly proportional to the layer weight fraction of the bed. The resulting layer dimensions used in this analysis are tabulated in Table 9.

The second approximation concerns the postboiling configuration of the debris bed. The thermocouple traces clearly indicate that the superheat disruption, which occurred early in the experiment, modified the bed configuration. Thermocouples 13, 14, 15, and 16 were not covered by debris after the disruption. This means that either the thermocouples were bent upward out of the bed or the debris originally covering these thermocouples was removed. This latter explanation is consistent with posttest X-ray photographs of the debris bed which show debris in the annulus outside of the crucible. Thermocouples B12 and B13 were located at 120 and 131 mm, respectively. It is therefore reasonable to assume that the top six layers of the bed were removed by the disruption and that the top of the bed was located at approximately 127.7 mm. It is also assumed that the stratification in the lower portion of the bed is unaltered, which is reasonable. Clearly, there is some mixing possible in the top layers of the disrupted bed, which is not accounted for in the calculations. As will be seen, predictions of dryout agree well with experimental dryout data if this modified configuration is assumed.

The first step in the data reduction is the calibration of the heat flux plate. This is done by analyzing the conduction runs tabulated in Table 3. In these runs, all energy generated below the adiabatic plane diffuses downward through the heat flux plate and radially through the crucible walls. For the purposes of calibration, these components are combined and divided by the area of the heat flux plate. This combined heat flux is plotted against the product of the thermal conductivity and the temperature difference across the heat flux plate (Figure 16). The result appears to be a linear relationship that can be adequately fitted by the equation

Table 9

Approximate D13 Layer Dimensions

Layer Number	Effective Particle Diameter (mm)	Weight Percent of Bed	Layer Thickness (mm)	Layer Elevation (mm)
1	2.451	3.59	5.74	5.74
2	1.992	3.54	5.66	11.40
3	1.511	2.79	4.46	15.86
4	1.326	3.25	5.20	21.06
5	1.080	3.58	5.73	26.79
6	0.936	3.91	6.26	33.05
7	0.768	4.26	6.82	39.87
8	0.667	4.60	7.36	47.23
9	0.547	4.90	7.84	55.07
10	0.472	5.20	8.32	63.39
11	0.390	5.27	8.43	71.82
12	0.334	5.35	8.56	80.38
13	0.276	5.36	8.58	88.96
14	0.236	5.40	8.64	97.60
15	0.198	5.02	8.03	105.63
16	0.168	4.65	7.44	113.07
17	0.140	4.60	7.36	120.43
18	0.119	4.55	7.28	127.71
19	0.101	3.97	6.35	134.06
20	0.0838	3.41	5.46	139.52
21	0.0707	3.13	5.01	144.53
22	0.0597	2.84	4.54	149.07
23	0.0482	3.33	5.33	154.40
24	0.0370	3.50	5.60	160.00

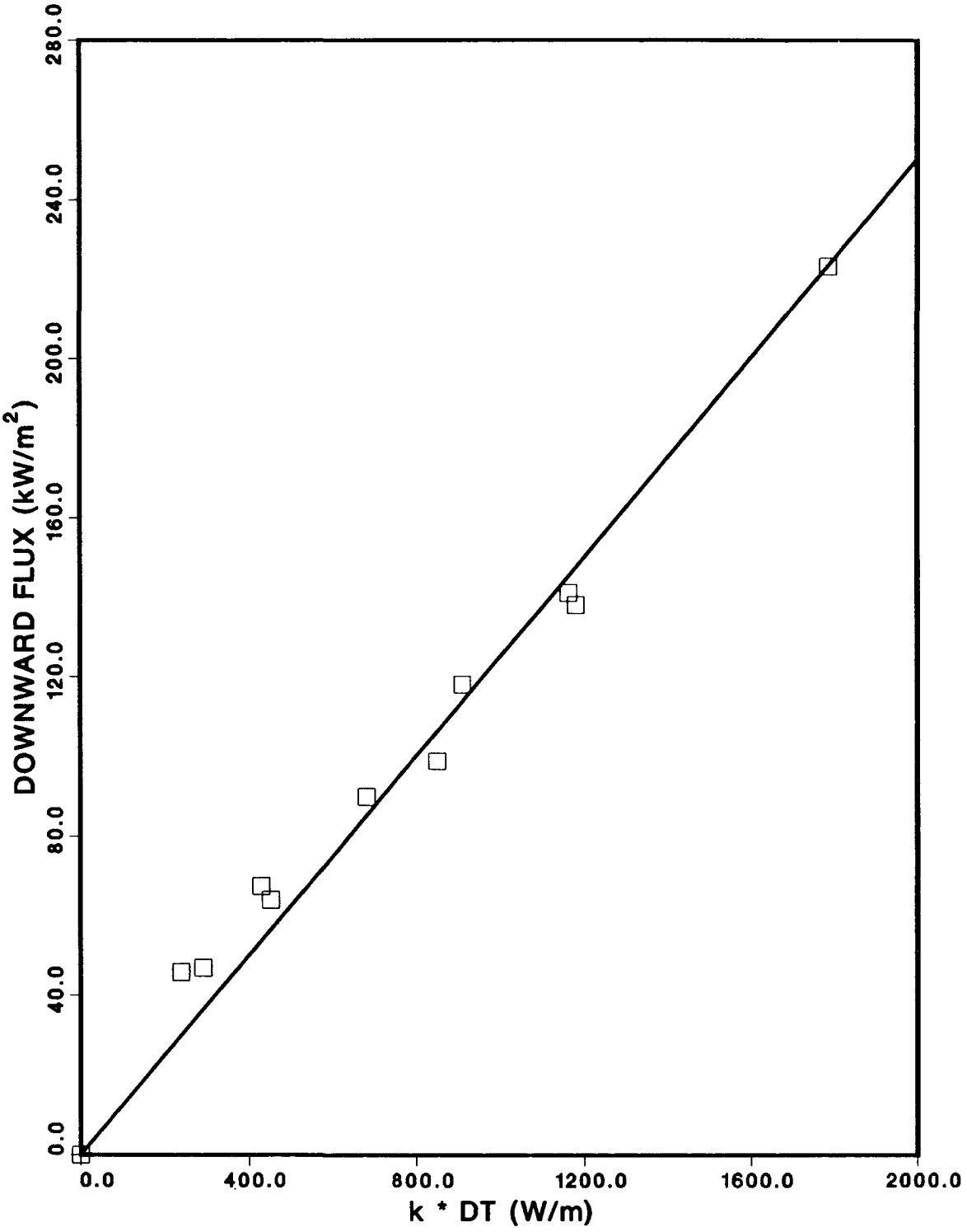

Figure 16. Downward Heat Flux Versus K·ΔT

$$Q_{down} = 125\ k\ \Delta T \quad ,$$

where Q_{down} is the downward heat flux in W/m^2, k is the thermal conductivity of the steel plate in W/m-K, and ΔT is the average temperature difference across the heat flux plate.

This downward heat flux calibration was applied to the incipient channeled dryout data (Table 10). The dryout data are shown with predictions of the Lipinski model in Figure 17. The solid line is the dryout prediction for the original 160-mm configuration assuming that the sticking factor for channel formation is unity; the dashed line is for complete channel suppression. These two lines diverge for a downward cooling of between 100 and 200 kW/m^2.

Unfortunately, the premature formation of channels by the superheat disruption eliminated the possibility of obtaining unchanneled data. However, incipient dryout data for the modified channeled configuration were obtained. The dotted line in Figure 17 is the Lipinski model prediction assuming that the top six layers were removed. The prediction for the modified configuration is between 30 and 50 percent greater than that of the original configuration and appears to be in reasonable agreement with the D13 data. Channeled dryout in the D10 experiment ranged from 1.06 to 1.5 W/g for a uniformly loaded bed with a full height of 160 mm. These values are comparable to the D13 results over similar amounts of bottom cooling. The maximum heat removal from the bottom of the D10 experiment was 450 kW/m^2, while bottom heat removal in D13 was up to 750 kW/m^2 as a consequence of the stratification enhanced downward boiling.

Further insight into the physics of dryout in stratified beds can be obtained by an examination of temperature profiles. Figure 18 shows the pre-dryout temperature profile of D01. Several things are clearly seen. Thermocouples B13, B14, B15, and B16 (elevations 131, 139, 148, and 154 mm, respectively) are at the pool temperature and are therefore not in the debris. Thermocouples B11 and B12 (elevations 109 and 120 mm, respectively) are subcooled but are hotter than the pool temperature. This indicates that they are still in the debris. Their responses to increases in reactor power confirm this.

Four relevant elevations have been marked on the figure. The bottom two lines mark the location of the adiabatic plane at powers of 0.86 and 0.94 W/g. This region of downward heat transfer is dominated by boiling. This demonstrates that downward boiling is taking place, and that its effect can be significant.

Table 10

Incipient Dryout Data

Dryout Number	Power Level (W/g)	C1/C2/C3 (°C)	C4/C5/C6 (°C)	$\Delta T/T_{avg}$ (°C/°C)	k (W/m-K)	Q_{down} (kW/m^2)
1	0.86- 0.94	693.1 661.7 668.4	820.4 785.3 777.8	127.3 123.6 109.4 ----- 120.1/ 734	18.1	272
6	2.15- 2.57	491.6 428.1 435.0	781.7 646.2 699.1	290.1 218.1 264.1 ----- 257.4/ 580	23.4	753
7	1.85- 2.58	471.2 405.7 434.9	697.2 653.5 630.6	226.0 157.8 195.7 ----- 193.2/ 534	22.5	543
8	1.46- 2.54	628.8 608.1 602.1	803.2 767.2 756.2	174.4 159.1 154.1 ----- 162.5/ 694	25.8	524
9	2.21- 2.61	562.0 551.7 523.7	785.2 768.0 718.9	223.2 216.3 195.2 ----- 211.6 652	24.9	659

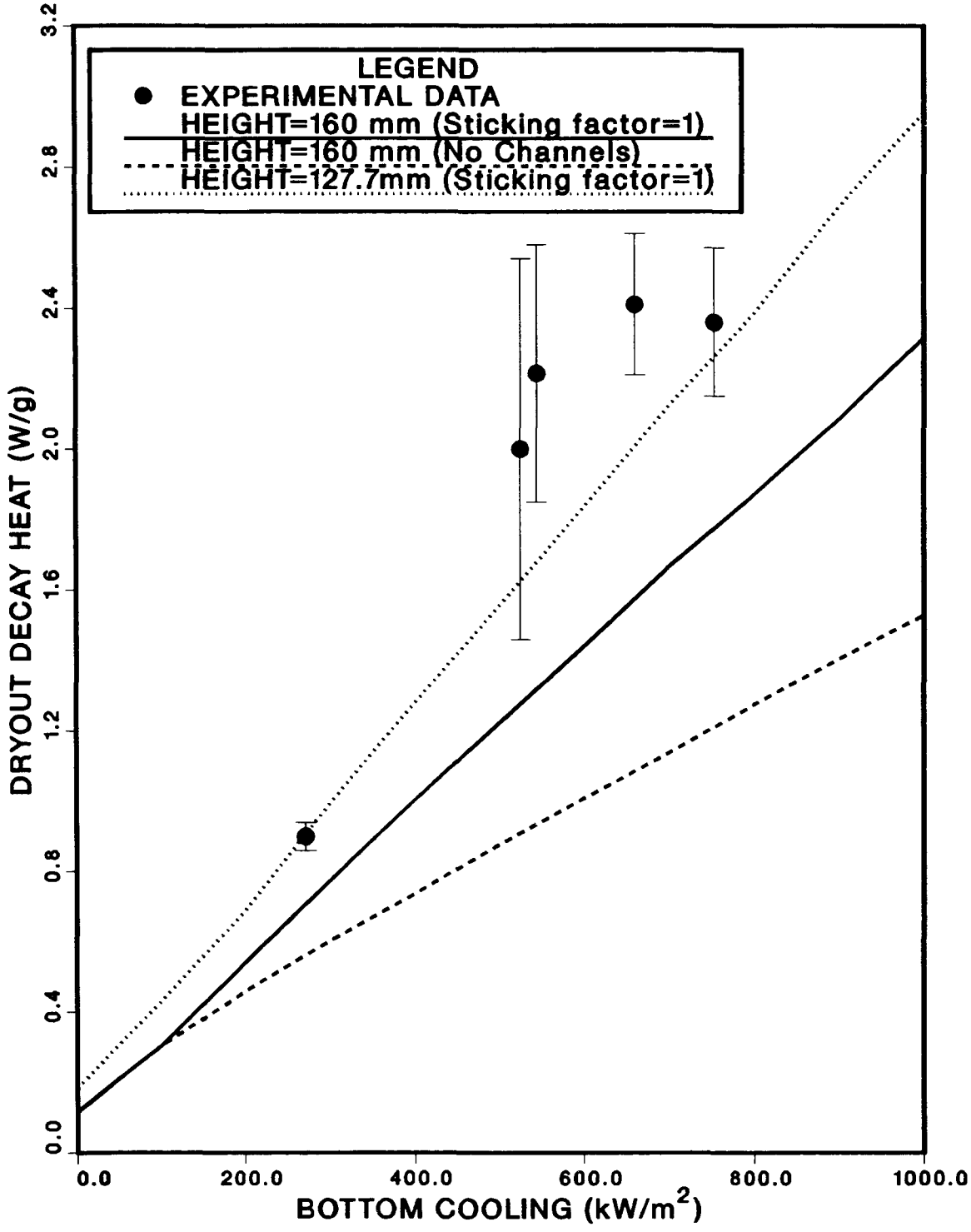

Figure 17. D13 Incipient Dryout Data Compared With Theory

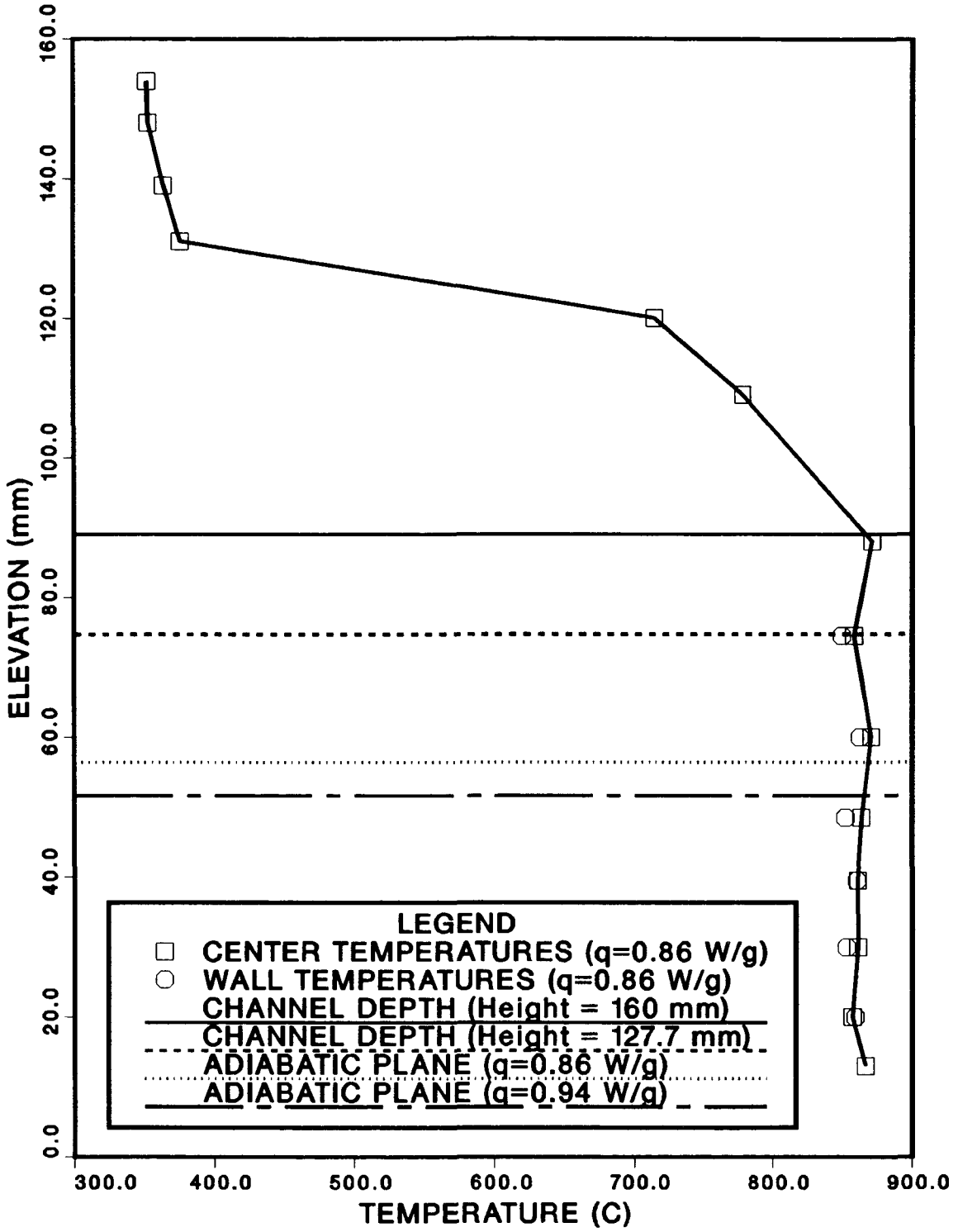

Figure 18. Predryout Axial Temperature Profile

The upper two lines are predictions of channel depth. The upper line is the predicted channel depth of the undisturbed 160-mm bed. The line below it is the prediction for the modified bed. In spite of the assumption that 32 mm of debris have been removed from the bed, the channel bottoms are only about 15 mm closer to the bottom of the bed. This is because the debris stratification partially offsets the debris removal.

It is interesting to note that the actual region of unchanneled upward boiling is quite narrow. This is due to the impact of stratification; even though the particles of adjacent strata are close in diameter, the jump in saturation at the stratification interface can be large. The average diameter ratio between adjacent strata is 1.20. The capillary pressure can be modeled by the relationship

$$P_c \sim d_p \, (1/S_{eff}-1)^{0.175} \, ,$$

where P_c, d_p, and S_{eff} are the capillary pressure, effective particle diameter, and effective saturation respectively. If the pressure changes across the individual layers are ignored, then the saturation jumps can be estimated by the relationship

$$\frac{d_{p,n-1}}{d_{p,n}} = \frac{(1/S_n-1)^{0.175}}{(1/S_{n-1}-1)^{0.175}} \, ,$$

where the subscript, n, refers to the layer number.

Table 11 shows the results of this calculation for a layer particle diameter ratio of 1.2. Over a set of five layers, the saturation drops from 70 to about 3 percent. Liquid-vapor counterflow contributes to this decline in saturation. Five layers represent only 20 percent of the bed. Hence, the region of rapid saturation decline can be quite small. It should be noted that this would also occur if the debris were continuously stratified. If this were the case, the saturation would decrease continuously instead of in jumps.

Table 11

Example of Saturation Jumps in D13

Layer Number	Saturation
n	0.7
n-1	0.452
n-2	0.225
n-3	0.093
n-4	0.035

5. SUMMARY AND CONCLUSIONS

The D13 experiment was the first fission-heated, stratified-debris coolability experiment to study the effects of bottom cooling, which might be provided by structural materials onto which the reactor debris might settle in an accident. This experiment was paired with the D10 experiment, which was essentially identical to D13 except that in D10 the bed was uniformly loaded without stratification. Hence, the two experiments were designed to examine the coolability of top and bottom cooled deep debris beds with and without stratified debris. Both experiments also looked at the coolability of such debris at very high temperatures approaching urania melt with sodium above and below the dry zone.

The D13 experiment was performed in two operations for over 40 hours with more than an hour at high temperature.

The initial operations included control runs, power calibrations, and urania wetting. A series of preboiling conduction/convection measurements were made with various bottom cooling rates. A second power calibration was performed before beginning the packed bed incipient dryout investigations. At the beginning of the boiling operations, the sodium in the bed superheated and subsequently flashed, disrupting the top of the bed such that the upper layers of the debris were trapped above the crucible leaving a channeled bed. A number of incipient dryout powers were measured for the channeled configuration. Also, several operations were performed that were designed to collapse the channels and regain a packed bed. The channeled configuration was unaltered.

The second part of the experiment was begun with a control run and a power calibration. The approach to boiling also resulted in a sodium superheat flash as did all such operations for the reason postulated earlier. An incipient dryout measurement was made and then three extended temperature operations were performed. This concluded the experiment. It should be noted that all of the mechanical hardware (containments, crucibles, etc.), the data acquisition system, and all instrumentation performed in an excellent fashion, and there were no failures during the conduct of the experiment.

The posttest X-rays revealed that the top portion of the bed had been removed consistent with the thermocouple results. The analysis of the modified channeled bed with the Lipinski model gave reasonable agreement. The experiment demonstrated that bottom cooling can be very effective in removing heat from debris. Based on the data, incipient

dryout powers are expected to increase an order of magnitude as compared to a bed with an adiabatic bottom boundary condition.

Bottom cooling can also overcome the adverse effects of stratification. The bottom heat removal in D13 was as high as 750 kW/m^2 as compared to 450 kW/m^2 in the D10 experiment.

6. REFERENCES

1. J. B. Rivard, Post-Accident Heat Removal: Debris Bed Experiments D-2 and D-3, Sandia National Laboratories, Albuquerque, NM, NUREG/CR-0421, SAND78-1238, 1978.

2. J. M. Gronager, M. Schwarz, and R. J. Lipinski, PAHR Debris Bed Experiment D-4, Sandia National Laboratories, Albuquerque, NM, NUREG/CR-1809, SAND80-2146, 1981.

3. G. W. Mitchell, R. J. Lipinski, and M. Schwarz, Heat Removal from a Stratified UO_2-Sodium Particle Bed, Sandia National Laboratories, Albuquerque, NM, NUREG/CR-2412, SAND81-1622, 1982.

4. G. W. Mitchell, C. A. Ottinger, and R. J. Lipinski, The D7 Debris Bed Experiment, Sandia National Laboratories, Albuquerque, NM, NUREG/CR-3198, SAND82-0062, 1983.

5. C. A. Ottinger, G. W. Mitchell, R. J. Lipinski, and J. E. Kelly, The D9 Experiment: Heat Removal from Stratified UO_2 Debris in Sodium, Sandia National Laboratories, Albuquerque, NM, NUREG/CR-2951, SAND84-1838, 1984.

6. G. W. Mitchell, C. A. Ottinger, and H. Meister, The D10 Experiment: Coolability of UO_2 Debris in Sodium With Downward Heat Removal, Sandia National Laboratories, Albuquerque, NM, NUREG/CR-4055, SAND84-1144, 1984.

7. C. P. Cannon, "2200°C Thermocouples for Nuclear Reactor Fuel Centerline Temperature Measurements," in Temperature: Its Measurement and Control in Science and Industry, Volume 5, J. F. Schooley, ed., (New York: American Institute of Physics, 1982).

8. C. P. Cannon, "Recent Advances in High Temperature Thermocouples," Proceedings of the Industrial Temperature Measurement Symposium, Knoxville, TN, September 10-12, 1984.

9. C. J. Greenholt and R. A. Sallach, "Water Adsorption by the Urania Bed in the D-Series Crucible ACRR Program," memo to J. E. Gronager, February 1, 1983.

10. T. R. Schmidt, "Power Distribution in the D-10 Debris Bed Experiment," memo to G. W. Mitchell, July 11, 1984.

11. K. Mehr, private communication, March 1985.

12. H. Nakamura, "Analysis of Temperatures in D10 Dryout Zones due to Instrumentation," Sandia National Laboratories, internal memorandum, October 20, 1983.

APPENDIX A

D13 Experimental Procedures

Startup

1. Electrically heat the sodium to 200°C. Do not exceed 35 V electrical power until sodium is at 120°C at S3.

2. Nuclear heating of the debris bed following melting of the sodium at a power of 0.16 W/g (90 kW ACRR Power).

Control Run

3. Initiate upward (nitrogen) cooling sufficient to maintain a sodium temperature of 350°C for a control run. No helium mass flow (minimum bottom cooling) would be used although there would be a finite downward heat flux.

Power Calibration

4. A power calibration run to establish the ratio of bed power to ACRR power, which is continuously recorded, would be accomplished by rapidly increasing power to 300 kW (600 kW scale), maintaining 300 kW for a period of about 2 minutes, and then reducing it back to 90 kW.

   Analyst--Determine coupling factor and bed conductivity.

Wetting of UO_2

5. Wetting of the UO_2 by the sodium is desirable to release trapped gas and insure a stable thermal response of the bed throughout the experiment. Wetting occurs more readily at high temperatures. Therefore, to achieve wetting, increase sodium temperature to 600°C using both electrical and nuclear heating. Adjust power to insure that maximum bed temperatures are less than 800°C. Helium cooling flow would be turned off. Temperatures below the heat flux plate (C1 and C2) should stabilize at about 650°C. Hold maximum temperatures for 1 hour. This procedure also serves as a 600°C control run.

   Analyst--Determine bed conductivity vs elevation, compare with conductivity from step 4.

Conduction/Single-Phase Convection

6. In order to establish various subcooled temperature profiles in the bed at different amounts of downward

heat removal, increase downward cooling to achieve C1/C2 temperatures of 450°C and 300°C at constant bed power and a sodium temperature of 600°C.

Analyst--Determine helium cooling capability as a function of C1/C2 temperatures.

7. At a sodium temperature of 600°C and with C1/C2 at 300°C, increase bed power until maximum temperatures are near 800°C.

   Analyst--Helium cooling vs C1/C2 temperature.

8. Reduce bed power to the control run power (90 kW). Reduce sodium temperature to 350°C, maintaining C1/C2 at 300°C.

9. Decrease downward cooling to achieve C1/C2 temperatures of 450°C and 650°C, at constant bed power and a sodium temperature of 350°C (second 350°C Control Run).

   Analyst--Determine bed conductivity vs elevation. Compare with previous data, provide to experimenter.

10. Conduct second power calibration at a sodium temperature of 350°C (90 to 300 kW).

    Analyst--Determine coupling factor.

11. Increase power in two steps with C1/C2 at 650°C to establish stable temperature profiles with maximum temperatures between 750° and 800°C.

Two-Phase Heat Removal/Packed Bed Incipient Dryout

12. In order to study heat transfer by boiling, establish C1/C2 temperatures of 700°C and increase power until boiling is observed (about 860°C). Increase power slightly in two steps to establish thicker stable boiling regions.

    Analyst--Determine desired power steps.

13. Continue to increase power until dryout is observed and until dryout extends to the walls of the crucible. To maintain crucible and instrumentation temperatures well within their capabilities, limit measured temperatures to 1200°C. If channeling is observed before reaching a packed bed dryout temperature of 1200°C, reduce power to reestablish a packed bed dryout and continue to step 14.

14. Reduce power to quench dryout and reestablish boiling. Increase downward cooling to achieve C1/C2 temperatures of 500°C and 300°C. Increase power to establish packed bed dryout for each downward cooling condition. Reduce power to quench dryout between steps.

Subcooling Effects on Packed Bed Dryout

15. Increase sodium temperature to 600°C. Increase bed power with C1/C2 at 700°C until dryout is observed and extends to the crucible walls. Limit measured temperatures to 1200°C. If channel penetration occurs, reduce power to reestablish packed bed dryout.

16. Reduce power to quench dryout and reduce the size of the boiling region. Increase downward cooling to achieve C1/C2 temperatures of 500°C and 300°C. Increase power to establish packed bed dryout for each downward cooling condition. Quench dryout between steps.

Extended Dryout Investigations

17. Reduce sodium temperature to 350°C. Establish boiling with C1/C2 at 300°C or the lowest temperature which can be maintained during higher power operations due to limitations in cooling capability. Increase power in small steps to achieve several steady-state dry zone thicknesses above incipient dryout power. Limit power or temperature to maintain subcooled zone thickness required to avoid channels or until a maximum bed temperature of 2000°C is achieved. Limit maximum temperatures to 2000°C to avoid UO_2 sintering. If channeling occurs, reduce power and reestablish incipient dryout to determine if channeling is reversible.

18. Quench the dry zone by reducing power. Decrease downward cooling to increase C1/C2 temperatures to 700°C. Increase power in small steps to establish several steady-state dryout zone thicknesses above incipient dryout.

19. Quench dry zone by reducing power. Increase sodium temperature to 600°C with C1/C2 at 700°C. Increase power in small steps to establish several steady-state dry zones above incipient dryout.

20. Quench dry zone by reducing power. Increase downward cooling to decrease C1/C2 temperatures to 300°C or lowest practical temperature. Increase power in small steps to establish several steady-state dry zones above incipient dryout.

Note: If channeling has already occurred, continue on to high temperature extended dryout; if not, continue with channeling investigations.

Channeling Investigations

21. Reduce power to quench dryout. At a sodium temperature of 600°C and with C1/C2 temperatures at 300°C, increase power in a slow ramp of about 0.1 W/g per minute to avoid a bed disruption. If channeling occurs prior to reaching a temperature limit of 2000°C, reduce power to determine if channeling is reversible.

22. Reduce power to quench dryout and decrease downward cooling to achieve C1/C2 temperatures of 700°C. Increase power in a slow ramp and observe for channeling.

23. Reduce power to quench dryout. Reduce sodium temperature to 350°C with C1/C2 at 700°C. Increase power in a slow ramp and observe for channeling.

24. Reduce power to quench dryout. Increase downward cooling to achieve C1/C2 temperatures of 300°C. Increase power in a slow ramp and observe for channeling.

High Temperature Extended Dryout

25. Repeat steps 21 to 24 in reverse order with a fast power ramp to 1.0 W/g within 20 seconds. Adjust power to achieve maximum bed temperatures of 2600°C.

Control Run

26. Reduce power to establish a nonboiling control run at a sodium temperature of 350°C with no helium flow.

27. Conduct third power calibration at 350°C.

28. Shutdown.

D13 Experimental Procedures

Session 2

1. Electrically heat the sodium to 200°C. Do not exceed 35 V electrical power until sodium is at 120°C at S3.

2. Nuclear heating of the debris bed following melting of the sodium at a ACRR power of 120 kW.

3. A control run will be accomplished at a sodium temperature of 600°C and minimum bottom cooling (700°C on C1/C2) and power calibration.

4. Cool bottom to 500°C. Shut down reactor. Lift experiment package approximately 1 inch and set back down. Repeat several times.

5. Restart reactor. Repeat control run 3 and power calibration.

6. Increase bottom cooling (C1/C2 400°C). Sodium temperature remains at 600°C for this control run.

7. Increase nitrogen cooling to achieve a sodium temperature of 350°C. Maintain bottom temperature of 400°C for this control run.

8. Decrease bottom cooling to achieve a bottom temperature of 700°C. Maintain sodium temperature of 350°C for this control run.

9. With sodium temperature of 350°C and bottom temperature of 700°C, increase power until either boiling is observed or the maximum bed temperature is no greater than 20°C above the expected boiling temperature of 860°C.

10. If boiling is not observed in 9, then increase sodium temperature to 600°C and cool the bottom to 400°C. Increase power until boiling is observed or the maximum bed temperature is no greater than 20°C above the expected boiling temperature of 900°C.

11. If boiling has not been observed, try to achieve a small superheat flash by applying a power step. Maintain boiling.

12. Increase nitrogen flow to cool sodium to 350°C. Decrease bottom cooling to achieve a bottom temperature of 700°C. Increase power until dryout is observed (limit power to approximately 1 MW). (Allow sodium

temperature to increase toward 600°C as maximum nitrogen cooling capacity is reached.)

13. If dryout power is low, indicating a packed bed, proceed with extended dryout investigations (steps 18, 19, 20 and 17 in original procedures).

14. If dryout power is high (greater than 1 MW), increase sodium temperature to 650°C and cool bottom to 500°C and stabilize. Increase nitrogen and helium cooling to maximum and increase reactor power to 1.9 MW. Limit sodium temperature to 675°C by reducing reactor power.

15. Repeat 14 with a subcooled bed (600°C).

16. Reduce power to establish a nonboiling control run at a sodium temperature of 350°C and a bottom temperature of 700°C and power calibration.

17. Shutdown.

DISTRIBUTION:

U.S. Government Printing Office
Receiving Branch (Attn: NRC Stock)
8610 Cherry Lane
Laurel, MD 20707
(200 copies for R7)

Division of Reactor Safety Research (14)
Office of Nuclear Regulatory Research
U.S. Nuclear Regulatory Commission
Washington, DC 20555
Attn: E. S. Beckjord
C. N. Kelber
T. L. King
R. M. Meyer
B. M. Morris
D. R. Ross
M. Silberberg
R. W. Wright (5)
G. Marino
P. M. Wood

Joint Research Center (10)
Ispra Establishment
21020 Ispra (Varese)
Italy
Attn: R. Klersy
K. Mehr
P. Fasoli-Stella
O. Simoni (5)
P. Schiller
H. Meister

Power Reactor & Nuclear Fuel
Development Corporation (PNC) (6)
Fast Breeder Reactor Development
Project (FBR)
9-13, 1-Come, Akasaka
Minato-Ku, Tokyo
Japan
Attn: A. Watanabe (2)
H. Nakamura
M. Saito
K. Takahashi
A. Furutani

Belgonucleaire
Rue du Champ de Mars 25
B-1050 Brussels, Belgium
Attn: J. Basselier

S.C.K./C.E.N.
Boeretang 200
B-2400 MOL
Belgium
Attn: C. J. M. Foly

Monsieur A. Schmitt
IPSN/DSN
CEN Fontenay-aux-Roses
B.P. 6
92260 Fontenay-aux-Roses
France

Safety Studies Laboratory/DSN (6)
Commissariat a L'Energie Atomique
Centre d'Etudes Nucleaires de Cadarache
B.P.1, 13115 Saint-Paul-lez-Durance
Bouches-du-Rhone
France
Attn: M. Schwarz
M. Bailly
M. Meyer Heine
M. Penet
G. Kayser
C. LeRigoleur

Centre d'Etudes Nucleaires
de Grenoble (2)
B.P. 85-Centre de Tri
38401 Grenoble Cedex
France
Attn: M. Costa/STT
D. Rousseau/Pi-SEDTI

UKAEA (2)
Safety and Reliability Directorate
Wigshaw Lane
Culcheth
Warrington, WA3 4NE
United Kingdom
Attn: M. Hayns
R. S. Peckover

Atomic Energy Establishment (6)
Winfrith, Dorchester
United Kingdom
Attn: R. V. Macbeth
R. Potter
G. L. Shires
G. F. Stevens
R. Trenberth
T. Butland

Culham Laboratory (3)
Culham
Abingdon
Oxfordshire OX14 3DB
United Kingdom
Attn: F. Briscoe
B. Turland
K. A. Moore

Kernforschungszentrum Karlsruhe (7)
D-75 Karlsruhe
Postfach 3640
West Germany
Attn: G. Heusener (PSB)
H. Werle (INR)
L. Barleon (IRB)
G. Hoffman (IRM)
K. Thomauske (IRB)
U. Muller (IRM)
G. Fieg (INR)

University of California (2)
Energy and Kinetics Department
Rm. 5405 Bolter Hall
Los Angeles, CA 90024
Attn: I. Catton
U. K. Dhir

Argonne National Laboratory (5)
Reactor Analysis and Safety Division
9700 South Cass Avenue
Argonne, IL 60439
Attn: L. Baker, Jr.
J. C. Cassulo
J. D. Gabor
R. D. Pedersen
E. S. Sowa

General Electric Company
6835 Via del Ora
San Jose, CA 95119
Attn: E. Gluekler

Westinghouse Electric Corp. (2)
Power Systems
P.O. Box 355
Pittsburgh, PA 15230
Attn: L. Hochreiter
D. Squarer

Westinghouse Research and Development Center
Pittsburgh, PA 15235
Attn: A. Pieczynski

Westinghouse Hanford Co. (2)
337 Bldg., 300 Area
P.O. Box 1970
Richland, WA 99352
Attn: G. R. Armstrong
C. P. Cannon

Nuclear Safety Analysis Center
3412 Hillview Avenue
P.O. Box 10412
Palo Alto, CA 94303
Attn: G. Thomas

Fauske and Associates (2)
631 Executive Dr.
Willowbrook, IL 60521
Attn: M. Epstein
R. Henry

Brookhaven National Laboratories (2)
Fast Reactor Safety
Upton, Long Island, NY 11973
Attn: J. W. Yang
T. Ginsberg

Los Alamos National Laboratories
Q7, Slot K556
Los Alamos, NM 87545
Attn: Javiei Escamilla

NUS Corporation
Consulting Division
4 Research Place
Rockville, MD 20850
Attn: Juan M. Nieto

EG&G, Idaho (3)
P. O. Box 1625
Idaho Falls, ID 83415
Attn: C. Allison
D. Croucher
R. W. Miller

Mass. Inst. of Tech. (2)
Mech. Eng. Dept.
Cambridge, MA 02139
Attn: P. Griffith
M. Kazimi

University of New Mexico
Nuclear Engineering Department
Albuquerque, NM 87131
Attn: M. El-Genk

University of Wisconsin (2)
Department of Nuclear Engineering
Madison, WI 53706
Attn: M. L. Corradini
S. Abdel-Khalik

University of California
Chemical and Nuclear Eng. Dept.
Santa Barbara, CA 93106
Attn: T. Theofanous

SANDIA DISTRIBUTION:

1274 R. J. Lipinski
1652 G. W. Mitchell (5)
3141 S. A. Landenberger (5)
3151 W. L. Garner
6222 K. R. Boldt
6320 J. E. Stiegler
6322 J. M. Freedman
6322 C. A. Ottinger (5)
6400 D. J. McCloskey
6410 N. R. Ortiz
6420 J. V. Walker
6421 P. S. Pickard
6421 D. N. Cox
6422 D. A. Powers
6422 R. D. Gomez
6423 K. O. Reil
6425 W. J. Camp
6425 J. E. Kelly
6425 A. W. Reed
6427 M. Berman
6440 D. A. Dahlgren
6450 T. R. Schmidt (5)
6451 T. F. Luera
6452 J. W. Bryson
6454 G. L. Cano
8024 P. W. Dean

NRC FORM 335 (2-84) NRCM 1102, 3201, 3202

U.S. NUCLEAR REGULATORY COMMISSION

BIBLIOGRAPHIC DATA SHEET

SEE INSTRUCTIONS ON THE REVERSE

1 REPORT NUMBER (Assigned by TIDC and Vol No. if any)

NUREG/CR-4719
SAND86-1043

2 TITLE AND SUBTITLE

Coolability of UO_2 Debris in Sodium with Downward Heat Removal: The D13 Experiment

3 LEAVE BLANK

4 DATE REPORT COMPLETED

MONTH: July — YEAR: 1986

5 AUTHOR(S)

C. A. Ottinger
G. W. Mitchell
A. W. Reed
H. Meister

6 DATE REPORT ISSUED

MONTH: March — YEAR: 1987

7 PERFORMING ORGANIZATION NAME AND MAILING ADDRESS (Include Zip Code)

ACRR Reactor-Safety Experiments
Sandia National Laboratories
Albuquerque, NM 87185

8 PROJECT TASK WORK UNIT NUMBER

9 FIN OR GRANT NUMBER

A-1181

10 SPONSORING ORGANIZATION NAME AND MAILING ADDRESS (Include Zip Code)

Nuclear Regulatory Research
U.S. Nuclear Regulatory Commission
Washington, DC 20555

11a TYPE OF REPORT

Technical

b PERIOD COVERED (Inclusive dates)

Jan. 1983 - Dec. 1985

12 SUPPLEMENTARY NOTES

13 ABSTRACT (200 words or less)

The LMFBR Debris Coolability Program at Sandia National Laboratories investigates the coolability of particle beds that may form following a severe accident involving core disassembly in a nuclear reactor. The D series experiments utilize fission heating of fully enriched UO_2 particles submerged in sodium to realistically simulate decay heating. The D13 experiment is the first in the series to study the effects of bottom cooling of stratified debris, which could be provided in an actual accident condition by structural materials onto which the debris might settle. Additionally the D13 experiment was designed to achieve maximum temperatures in the debris approaching the melting point of UO_2. The experiment was operated for over 40 hours and investigated downward heat removal at specific powers of 0.22 and 2.58 W/g. Channeled dryout in the debris was achieved at powers from 0.94 to 2.58 W/g. Maximum temperatures approaching 2700°C were attained. Bottom heat removal was up to 750 kW/m^2 as compared to 450 kW/m^2 in the D10 experiment.

14 DOCUMENT ANALYSIS - a KEYWORDS DESCRIPTORS

b IDENTIFIERS OPEN ENDED TERMS

15 AVAILABILITY STATEMENT

16 SECURITY CLASSIFICATION
(This page)
(This report)

17 NUMBER OF PAGES

18 PRICE

☆ U.S. GOVERNMENT PRINTING OFFICE 1987—773-049/41042